Noble Metal Nanomaterials for NIR-Triggered Photothermal Therapy in Cancer

Zhuoqian Lv, Sijia He, Youfu Wang,* and Xinyuan Zhu

It is of great significance to develop anticancer therapeutic agents or technologies with high degree of specificity and patient compliance, while low toxicity. The emerging photothermal therapy (PTT) has become a new and powerful therapeutic technology due to its noninvasiveness, high specificity, low side effects to normal tissues and strong anticancer efficacy. Noble metal nanomaterials possess strong surface plasmon resonance (SPR) effect and synthetic tunability, which make them facile and effective PTT agents with superior optical and photothermal characteristics, such as high absorption cross-section, incomparable optical-thermal conversion efficiency in the near infrared (NIR) region, as well as the potential of bioimaging. By incorporating with various functional reagents such as antibodies, peptides, biocompatible polymers, chemo-drug and immune factors, noble metal nanomaterials have presented strong potential in multifunctional cancer therapy. Herein, the recent development regarding the application of noble metal nanomaterials for NIR-triggered PTT in cancer treatment is summarized. A variety of studies with good therapeutic effects against cancer from impressive photothermal efficacy of noble metal nanomaterials are concluded. Intelligent nanoplatforms through ingenious fabrication showing potential of multifunctional PTT, combined with chemo-therapy, immunotherapy, photodynamic therapy (PDT), as well as simultaneous imaging modality are also demonstrated.

1. Introduction

For centuries, malignant tumor, namely cancer, has been one of the main diseases that threaten the health of human.[1,2] At present, the treatment of cancer is mainly limited to surgery, chemotherapy, and radiotherapy. Surgery is the only way to remove the cancer from human body, but it could not remove small or minor lesion that is invisible to the naked eye. The

Z. Lv, Dr. Y. Wang, Prof. X. Zhu
School of Chemistry and Chemical Engineering
Frontiers Science Center for Transformative Molecules
Shanghai Jiao Tong University
800 Dongchuan Road, Shanghai 200240, China
E-mail: wyfown@sjtu.edu.cn
Dr. S. He
Cancer Center
Shanghai General Hospital
Shanghai Jiao Tong University School of Medicine
650 Xinsongjiang Road Shanghai 201620, China

The ORCID identification number(s) for the author(s) of this article can be found under https://doi.org/10.1002/adhm.202001806

other two methods can kill cancer cells effectively, while causing prominent damage to normal tissues.[3–6] With great potential to address these hurdles, photothermal therapy (PTT) has captured widespread attention due to its strong anti-cancer effect, high specificity, low invasiveness, and low side effects to normal tissues.[7–9]

It has been reported that when the temperature of cancer site is higher than 42 °C,[10] cancer cells can be effectively killed. PTT is an emerging thermal treatment to ablate cancer cells. During PTT, the temperature change of cancer site is caused by the medium that converts light energy into heat energy, which is called photothermal agent. Utilizing the heat tolerance variance between cancer cells and normal cells, high temperature can kill cancer cells and avoid obvious side effects on normal cells nearby. Specifically, photothermal agents are first concentrated in the lesion site and then irradiated with light. Subsequently, the photothermal agents generate a lot of heat to destroy the cancer cells in the lesion site. Near infrared (NIR) light is widely used in the study of PTT due to its superior tissue penetration and capability of remote control. In addition, it has high-resolution adjustment of time and space, which makes it precisely controlled.

Photothermal agent has a suitable NIR bandgap and can respond to the irradiation of NIR light. The ideal photothermal agents should have strong absorption in the NIR region, and can effectively convert the absorbed light energy into heat energy. In addition, they should be low toxic or nontoxic with good biocompatibility. In recent years, a variety of nanomaterials with strong NIR absorption, such as noble metal nanomaterials, graphene and analogues nanomaterials,[11] transition metal chalcogenides,[12–14] semi-conducting polymer nanoparticles,[15,16] have shown great potential in cancer therapy due to their high photothermal conversion efficiency (PCE).

Because of the strong surface plasmon resonance (SPR) effect and synthetic tunability, noble metal nanomaterials have been considered as facile and effective PTT agents with superior optical and photothermal characteristics, such as high absorption cross-section, incomparable PCE in the NIR region, as well as the potential of bioimaging.[17,18] By fabricating with other functional reagents such as antibodies, peptides, biocompatible polymers, chemo-drug and immune factors, noble metal

**ADVANCED
SCIENCE NEWS**

www.advancedsciencenews.com

**ADVANCED
HEALTHCARE
MATERIALS**

www.advhealthmat.de

nanomaterials have presented strong potential in multifunctional cancer therapy.[19]

Featuring the distinct photophysical property of strong SPR, noble metal nanomaterials have stood above the other types of photothermal agents. By utilizing laser irradiation with a frequency resonant with the absorption of nanomaterials, free electrons of the noble metal oscillate coherently around the nanoparticle surface. The nonradiative extinction caused by absorption and scattering can be converted to localized heat efficiently via electron-electron and electron-phonon relaxations on the order of a picosecond timescale.

Considering that it is desirable for noble metal nanomaterials to have SPR band in the NIR region, factors that affect the surface charge density, such as size, shape, structure, and the dielectric properties of the metal and the surrounding medium, can be properly modified to achieve the purpose. For example, hollow or core–shell nanostructures exhibit a red shifted SPR contrary to the solid ones. Anisotropic nanoparticles, such as rods, cages, triangles, sheets, and branched structures can also have strong absorption in the NIR region.[17]

Due to the rapid development of NIR trigged noble metal nanomaterials as PTT agents for PTT and no comprehensive review on this topic involving various noble metals, we will focus on the recent advances in the noble metal (Au, Ag, Pd, and Pt) nanomaterials as photothermal agents in NIR-triggered PTT and also involve related multimodal theranostics. To provide researchers with related information and reference, a variety of studies with good therapeutic effects against cancer from impressive photothermal efficacy of noble metal nanomaterials have been concluded. Moreover, intelligent nanoplatforms through ingenious fabrication showing potential of multifunctional PTT, combined with chemo-therapy, immunotherapy, photodynamic therapy (PDT), as well as simultaneous imaging modality were also demonstrated.

2. Gold Nanomaterials

The most explored noble metal nanomaterials in PTT are gold nanomaterials, possessing the advantages of enhanced absorption, excellent photostability, tunable physical and optical property, high biocompatibility, great heating effect deriving from rich free electrons.[20] There have been several kinds of gold nanomaterials with unique sizes and morphologies (nanorods, nanospheres, nanostars, nanocages, nanoshells, etc.), to achieve a strong NIR absorption and meet certain functional demands, all of which will be exhibited below.

2.1. Gold Nanorods

With tunable aspect ratio (length/width), small-size gold nanorods (GNRs) are effective PTT agents owning a large absorption cross section and a narrow absorption spectrum which results from the dramatic reduction of radiation attenuation effect.[21–23]

Compared with other gold nanomaterials, GNRs with elongated morphology can accumulate in cancer lesion and enter into cells more rapidly because of extraordinary transmembrane transport and diffusion rates.[24] Moreover, GNRs have

been proven to have better PTT effect than gold nanoshells as GNRs required lower laser intensity and excreted quicker from the body.[25] GNRs can also be utilized as NIR-responsive contrast agents for bioimaging with enhanced scattering property, which are promising theranostic platforms.[26] In 2006, Huang et al.[27] provided the first in vitro demonstration of GNRs' NIR-responsive PTT effect on cancer cells as well as their role as bioimaging contrast agents. Cell viability test showed that NIR laser at 800 nm and above 80 mW exposure killed malignant HaCat cells effectively. Moreover, with the conjugation of monoclonal antibodies, anti-epidermal growth factor receptor (anti-EGFR), the functional GNRs could specifically bind to malignant cells, which allows for precisely localized heating effect and 2-times increasement of cellular uptake, thus reducing unnecessary damage toward normal tissues and lowering the threshold irradiation energy to cause destruction of cancer cells to nearly half of that for normal cells.

Recently, small GNRs (30 nm × 7 nm) were fabricated through a one-spot seedless synthetic method and subsequently effectively endocytosed by macrophages, which act as biocompatible "Trojan horse" to help GNRs infiltrate cancer lesions and enhance their in vivo PTT efficacy.[28] Experiments proved that such small GNRs displayed higher cell uptake and less cytotoxicity than the common GNRs (56 nm × 14 nm). And in vivo PTT studies showed that, by treating with GNRs-laden-macrophages, the temperature of the cancer lesion increased from 34.5 to 44.3 °C in 1 min and reached as high as 53.8 °C after 10 min under 808 nm irradiation, finally reaching 95% cancer inhibition after two weeks. Their findings successfully explored the great potential of cell-mediated nanoagent therapies in clinical oncology.

2.2. Gold Nanospheres

Despite the lack of tunable SPR peak in the NIR region, gold nanospheres (GNSPs) can still non-radioactively absorb NIR light, by converting it to absorptive visible photons through second harmonic generation, and exhibit ideal photothermal effect, benefiting from the inherent nonlinear optical properties.[29] Moreover, GNSPs tend to aggregate through electrostatic interaction in colloid solution, which can further enhance the NIR absorption.[30] Nevertheless, gold aggregates could show broader SPR spectral range ascribed to inhomogeneous broadening of size and shape that is disadvantageous for delivery. Compared with other gold nanostructures, such as nanorods and nanoshells, GNSPs have no cytotoxic surfactant like CATB during nanofabrication, and better tumor uptake as well as more facile synthesis methods and bioconjugation strategies. For example, by conjugating to anti-EGFR antibodies, GNSPs were able to enter cancer cells selectively and exerted deadly thermal effect on cancer cells upon pulsed laser irradiation (800 nm), in which the laser energy was 20 times lower than the intensity used in the treatment without GNSPs.[29]

As a derivative, hollow GNSPs (HGNs) have attracted a particular interest with many advantages such as small size (30–50 nm), large interior space, high colloidal stability, strong and tunable SPR absorption in NIR region by adjusting outer diameter or shell thickness. Direct comparison with solid GNSPs reveals that owing to stronger NIR absorption and more
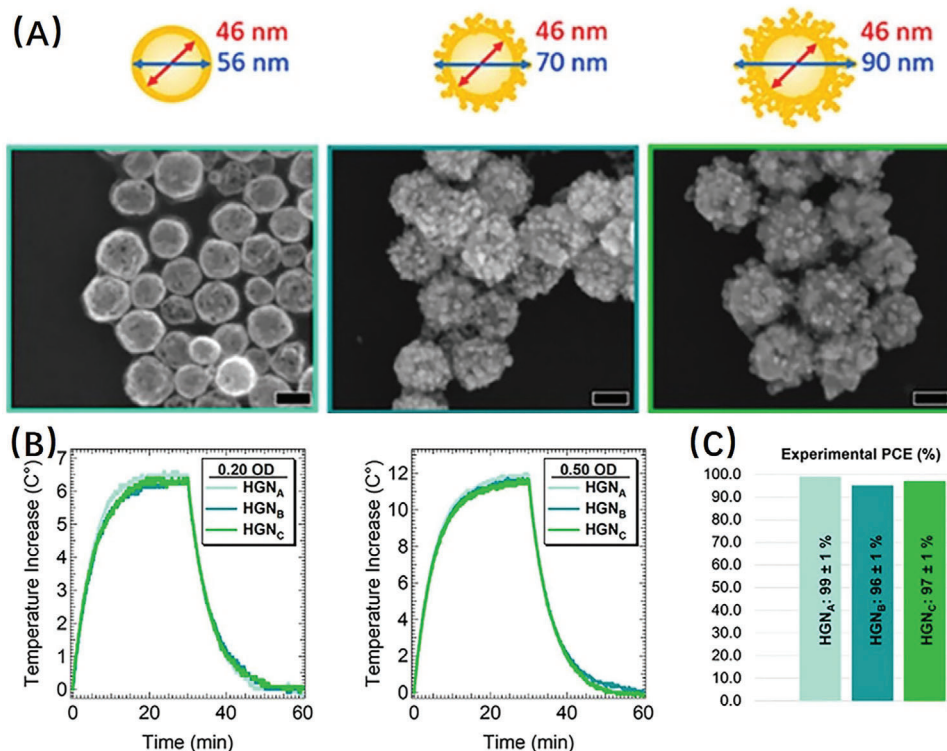
ADVANCED
SCIENCE NEWS

www.advancedsciencenews.com

ADVANCED
HEALTHCARE
MATERIALS

www.advhealthmat.de

Figure 1. A) Schematic demonstration of HGNs and related SEM images for HGN_A, HGN_B, and HGN_C with equivalent inner diameter, respectively. Scale bar = 50 nm. B) Temperature evolution curves for HGN_{A-C} with extinction optical density (OD) values at 0.20 and 0.50. C) Experimental PCE values for HGN_{A-C}. Reproduced with permission.[32] Copyright 2019, American Chemical Society.

effective photothermal conversion, HGNs are, at least, eight times more efficient in PTT.[31] The general synthesis route of HGNs is based on template fabrication using inorganic nanoparticles such as cobalt (Co) and silica as initial cores, without organic solvents and harsh surfactants. By attaching short peptide, NDP-MSH ([Nle⁴-D-Phe⁷]α–melanocyte-stimulating hormone), to PEGylated HGNs, receptor-mediated active targeted delivery of photothermal agents toward melanoma was achieved in a murine tumor model.[31] Histological experiments and [¹⁸F]fluorodeoxyglucose PET detection confirmed selective photothermal ablation of the melanoma cancer cells, suggesting great potential of HGNs for clinical photothermal treatment of cancer.

Recently, Lindley et al. examined the effect of surface rugosity on PCE of HGNs, whose surfaces were customized from smooth to bumpy by controlling the amount of NaOH added in the gold solution. Results showed that bumpy HGNs beat smooth counterparts in several aspects: ultra-high PCE up to 99%, enhanced surface area to load therapeutic drugs and enhanced local field for imaging as shown in **Figure 1**.[32]

The exceptionally large two-photon action cross-section ($\approx 1.02 \times 10^6$ GM at 820 nm) also makes HGNs available for deep tumor PTT triggered by femtosecond laser pulses with deep light penetration. Upon a mean power density of 1.6 W cm^{-2} and a total irradiation time of 81 μs, HGNs conjugated with folic acid (FA) can induce membrane blebbing and irreversible cell destruction by local, confined hyperthermia in the cancer lesion. Additionally, simultaneous cell imaging was realized under multiphoton

microscopy by HGNs, demonstrating a two-photon photoluminescence quantum yield of 1.5×10^{-4}, higher than any GNSPs reported to date.[33]

2.3. Gold Nanostars

Because of the sharp protruding tips surrounding the spherical core, gold nanostars (GNSTs) have strong confinement of the electric field and cause significant dephasing of coherently oscillated surface electrons, which can transfer to the atomic lattice and ultimately generate remarkable heat flux at the metal-dielectric interface.[34] Moreover, excessive exposure to GNSTs may harm normal cells, but are well avoided owing to the sharpness of multiple edges.

Advances in the synthesis of GNSTs have enabled experimental study into the optimum character and conditions for GNSTs to perform highly effective PTT. For example, by testing the heating effect of a series of GNSTs with average diameters from 25 to 150 nm and corresponding SPR peaks from 500 to 1000 nm within aqueous dispersion, cancer cells in vitro and solid tumors in vivo, respectively. Espinosa et al. found that both particle size of GNSTs and wavelength of irradiation laser can exert notable influence on heating effect in aqueous dispersion, while such relevance is markedly attenuated under in vitro and in vivo circumstances when GNSTs are internalized by cells and aggregated in endosomes (**Figure 2**).[35] Therefore, in addition to the
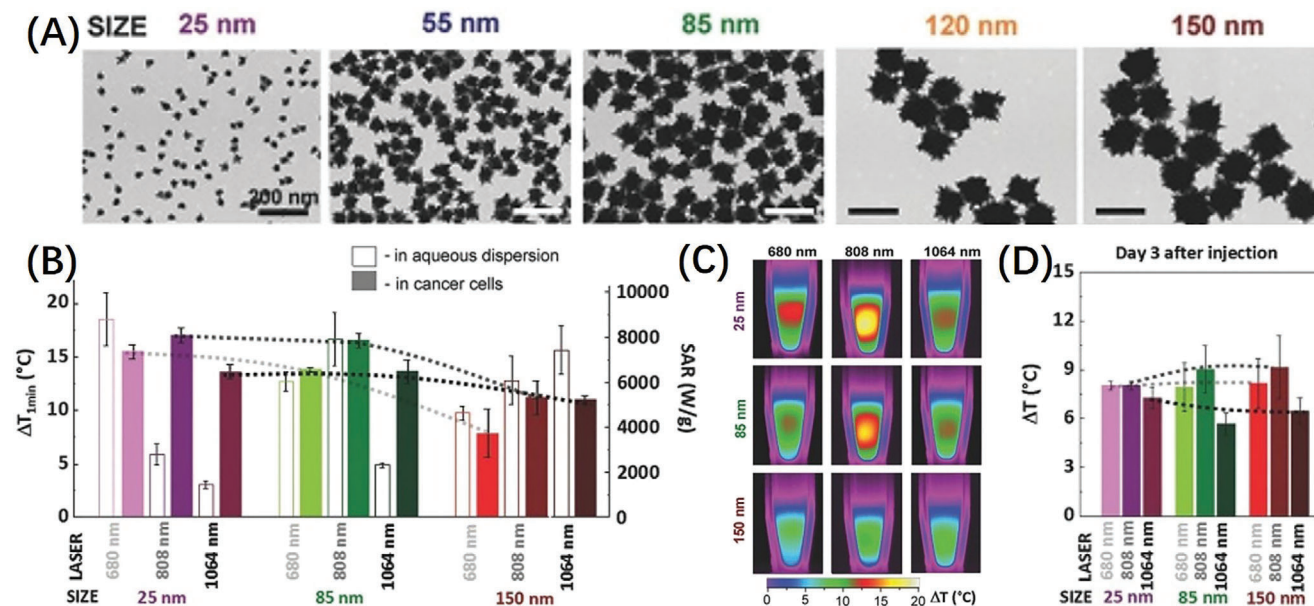
Figure 2. A) TEM images of five samples of GNSTs varying in size, scale bar = 200 nm. B) Average temperature increases of cell samples treated by GNSTs upon laser irradiation (1 W cm^{-2}, 1 min) at 680, 808, and 1064 nm. C) Thermographic images of cell samples, incubated with 25, 85, and 150 nm GNSTs from top to bottom, after exposure at 680, 808, and 1064 nm (1 W cm^{-2}, 1 min). D) Average temperature increases of tumors treated by GNSTs upon laser exposure (1 W cm^{-2}, 1 min) at 680, 808, and 1064 nm. Reproduced with permission.[35] Copyright 2016, Wiley-VCH GmbH.

facilitated biodistribution, it is concluded that the smallest GN-STs (25–50 nm) are superior candidates for in vivo PTT.

With a two-photon excitation cross-section several orders of magnitude greater than conventional organic dyes, GNSTs are also available for NIR-femtosecond-laser-triggered PTT along with in vivo highly resolved monitoring under multiphoton microscopy. Utilizing such advantage, Yuan et al. functionalized GNSTs with trans-activating transcription (TAT) peptide as shown in **Figure 3**A, which can boost cellular internalization through action-driven lipid raft-mediated micropinocytosis. The uptaken process of GNSTs can be monitored through two photon luminescence (TPL) as shown in Figure 3B,C.[36] In vitro experiments on BT549 breast cancer cells showed that, after 4 h treatment with TAT-GNSTs, large amounts of cells were damaged under ultralow irradiation intensity of 0.2 W cm^{-2} at 850 nm.

2.4. Gold Nanocages

Through galvanic replacement between silver nanocubes and chloroauric acid (HAuCl$_4$), gold nanocages (GNCs) with hollow interiors and porous exterior, can be easily synthesized. The SPR peak of GNCs could be precisely adjusted to NIR region by controlling the amount of HAuCl$_4$. These as-synthesized GNCs possessed absorption cross section five orders of magnitude higher than the organic fluorophores such as indocyanine green with a compact size of 40 nm for in vivo delivery.[37] In addition, the distinctive structures confer GNCs with drug loading capability and stimuli-responsive release feature, including pH, temperature and enzyme, which make it available to develop high-performance PTT with long agent-circulation time.[38]

Employing the more acidic extracellular microenvironment of cancers than normal tissues', a sufficiently pH sensitive

acylsulfonamide-based zwitterionic ligand was conjugated to GNCs via the thiol-Au reaction, intended to achieve a starkly longer systemic circulation life time and significantly targeted accumulation without active targeting moieties.[39] Upon the trigger of acidic pH around cancer cells, the "zwitterionic" ligands at physiological will reverse to "cationic" model, causing dynamic exchange that expose the particle's cationic surface to the proteins on cellular membrane and facilitate cellular internalization. Furthermore, cell viability tests revealed that, while promoting cellular uptake, pH-responsive ligand narrowly weakens the photothermal efficacy of GNCs, thus causing stronger cytotoxicity at acidic pH in cancer than other tissues.

Cancer-cell-targeted endocytosis and enzyme-responsive drug release enhanced PTT nanoplatform was developed by Wang et al., based on DOX (doxorubicin)-loaded GNCs capped with biodegradable hyaluronic acid (HA). After guiding DOX-GNCs to cancer lesion via specific interaction with overexpressed CD44 on cancer cells, HA could be degraded into nontoxic fragments by intracellular lysosomal enzyme hyaluronidase, which induces the leakage of DOX to destruct cancer cells. Meanwhile, after the irradiation of NIR laser, GNCs can efficiently transduce photons into heat, which causes cancer ablation and accelerates drug release, achieving synergistic chemo-photothermal therapy for solid tumors.[40]

2.5. Gold Nanoshells

Spherical gold nanoshells (GNSs), with a dielectric core larger than 100 nm, have been undoubtedly central among PTT agents developed in the last few years. In possession of many unique optical and chemical properties, GNSs are promising candidates in bioimaging and cancer therapy.[41] The maximum SPR
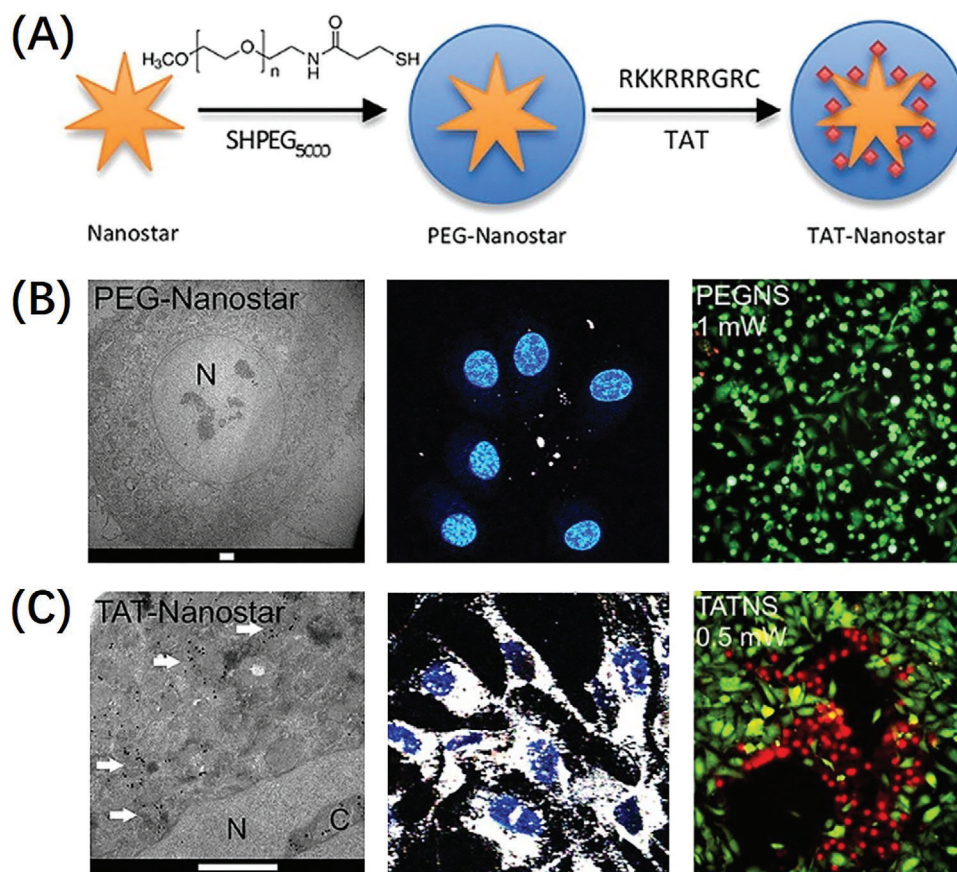
**ADVANCED
SCIENCE NEWS**

www.advancedsciencenews.com

**ADVANCED
HEALTHCARE
MATERIALS**

www.advhealthmat.de

Figure 3. A) Schematic diagram of the fabrication of functional gold nanostars. B,C) TEM, TPL and confocal microscope images of cell-uptaken PEG-Nanostar and TAT-Nanostar, respectively. TEM image scale bar = 2 µm, TPL images size = 125 × 125 µm², microscope image size = 625 × 625 µm². Reproduced with permission.[36] Copyright 2012, American Chemical Society.

absorption wavelength of GNSs can be preferentially tuned to 800–1200 nm by alternating the thickness of the shell since GNSs' plasmon hybridization becomes stronger when thickness increases and weaker the opposite.[42] Moreover, GNSs can passively accumulate in the tumor site through leaky tumor vasculature and actively target at specific cancer cells by conjugated to antibodies, proteins, or ligands.[43,44] In spite of these encouraging characteristics, it is still difficult to synthesis true GNSs in high quality, with proper size, spherical shape, and narrow SPR absorption.[45]

The spherical core–shell structure enables GNSs to load and deliver drugs efficiently, making them ideal candidates for multifunctional PTT, synergistically combined with chemotherapy, PDT, immunotherapy and so on. For example, by decorating with a thiol functionality, high-$^1O_2$-quantum-yield photosensitizers (PS) Pd[DMBil1]-PEG$_{5000}$ (linear tetrapyrole Pd complexes) was readily conjugated to the surface of silica core/gold shell (CS) as shown in **Figure 4**A, the safety of which has been established cynically.[46] Upon excited by a single wavelength of pulsed laser (800 nm, 1 W cm^{-2}), CS emit upconverted photoluminescence which activates PDT process of Pd[DMBil1]-PEG$_{5000}$, producing $^1O_2$ through luminescence resonance energy transfer-based sensitization. Meanwhile, complementary to PDT, local heat is generated oxygen-independently by GNSs, initiating cancer cell abla-

tion in hypoxic tissue, especially solid tumor. Effective anticancer effect of CS-PS has been reported to increase the level of reactive oxygen species (ROS), and a 40% apoptotic population without increase of necrosis.

As shown in Figure 4B, utilizing a micellar template self-assembled by PDMA-PCL copolymers, chemotherapeutic agent dichloro(1,2-diaminocyclohexane)platinum(II) (DACHPt) was directly loaded in the core domains in a sufficient dose and without pre-treatment. Then GNSs were fabricated within the shell domains of micellar templates. Moreover, GNSs, intended to produce a dramatic photothermal effect as well as inhibit premature drug release, were grown around the micellar surface, thus forming a highly biocompatible nanomedicine for chemo-photothermal therapy of colorectal cancer.[47]

Silica-cored GNSs are the first photothermal nanoparticles to enter clinical evaluation stages, appearing as AuroShell Particles in 2008.[48] Recently, a clinical pilot device study on AuroLase Therapy (Nanospectra Biosciences, Inc., Houston, TX), was carried out, which specifically suppress prostate tumors by GNSs-mediated heat ablation, combined with magnetic resonance-ultrasound fusion imaging technology.[49] The treatment worked effectively in 94% (15/16) of patients with feasible procedure and no negative complications.
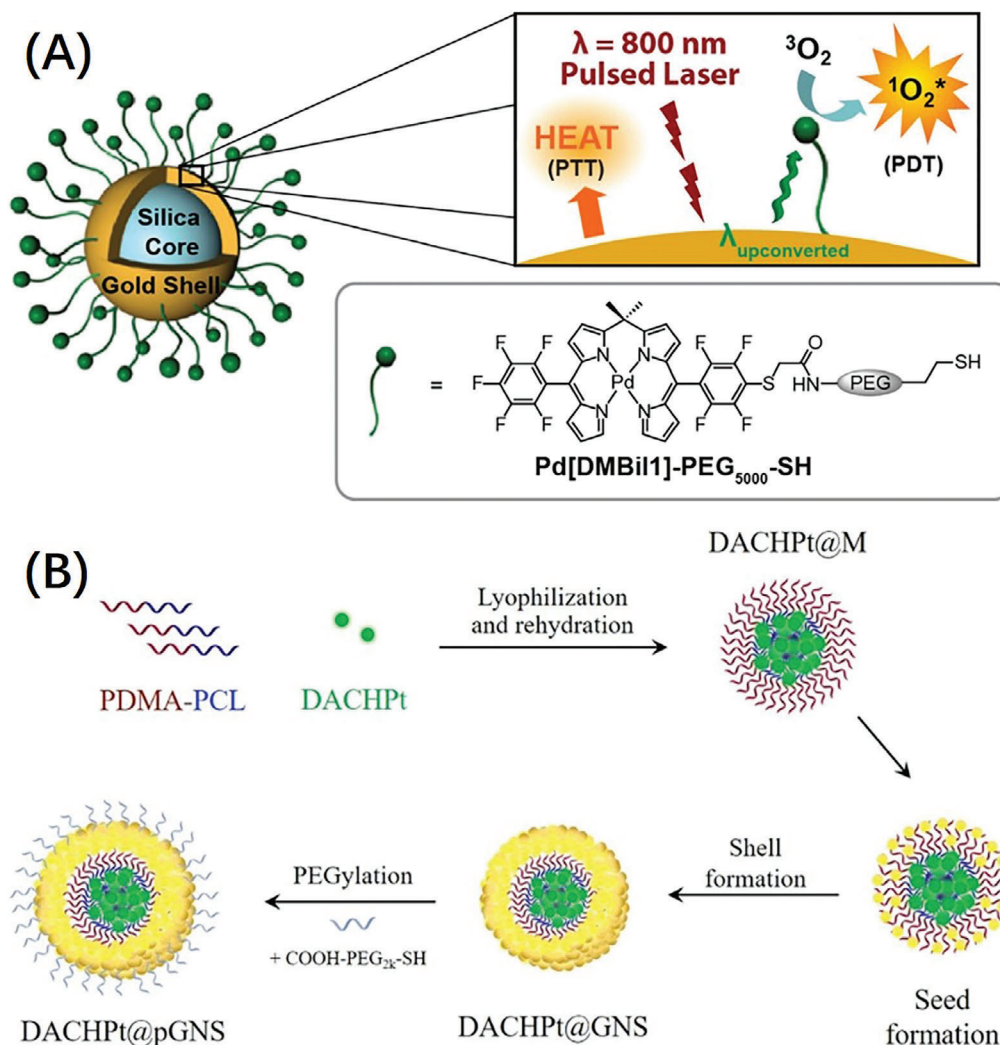
Figure 4. A) Schematic illustration of nanocomposites with photosensitizer Pd[DMBil1]-PEG$_{5000}$ and PTT agents GNSs and mechanism of NIR-triggered PDT and PTT. B) Fabrication diagram of Platinum (II) drug-loaded GNSs using PDMA-PCL micellar template for chemo-photothermal therapy in colorectal cancer. Reproduced with permission.[46,47] Copyright 2020, American Chemical Society.

2.6. Others

Except traditional gold nanomaterials mentioned above, some novel types of PTT agents based on gold are emerging incessantly, such as gold nanorings, gold nanoprisms,[50] gold caterpillar-like nanoparticles.[51]

Non-spherical nanostructures, such as plate-like and elongated nanoparticles (**Figure 5**A,C), can target tumors more efficiently than spherical ones by the restrain of mononuclear phagocyte system interaction and the tendency of margination in blood vessels. 2D gold nanorings as shown in Figure 5B have been finely fabricated for photoacoustic imaging and PTT via selective gold deposition on the edges of silver nanoplates and a second gold deposition following silver etching. Compared with gold nanospheres and nanoplates, gold nanorings display higher accumulation in tumors and lower uptake by macrophages cells, which may attribute to the distinct surface areas and high curvature at the edges.[52]

Interestingly, a distinctive kind of octopus-shaped gold nanoparticles with a mesoporous silica shell and Au branches as shown in Figure 5D is sophisticatedly synthesized by Zhang et al.,[53] modified with steric stabilizer PEG for their biocompatibility improvement and lactobionic acid (LA) for specific targeting. After loaded with DOX, the complex nanoarchitectures can be applied in pH-NIR dual-responsive chemo-photothermal therapy.

Because of the strong SPR effect, gold nanomaterials are pretty ideal photothermal agents. The properties and performances of various gold nanomaterials used in PTT are summarized in **Table 1**. During the various nanostructures of gold nanomaterials, small, flat, or elongated plasmonic nanostructures are more suitable for the light absorption and the subsequent heat generation, even with the same volume. This may due to that the inner and outer parts of the particle are close to each other, so an incoming electric field can penetrate deeply inside the thin nanostructure and involve the entire volume of the nanostructure

Table 1. The properties and performances of various gold nanomaterials used in PTT.

Types of Gold	Materials	Size	Laser Irradiation	ΔT [°C]	PCE	Additional Functionalities	Ref.
Gold nanorods	GNRs laden macrophages	7 × 13 nm	808 nm (1.0 W cm^{-2}, 60 s)	9.8 °C (in vivo)	21%	High cell uptake	[28]
	GNRs@TAT-peptide	10.5 × 40.5 nm	808 nm (0.2 W cm^{-2} 300 s)	≈2 °C (in vivo)		Nuclear targeted delivery via TAT-peptide	[21]
	GNRs@C	50 nm (10 nm shell)	808 nm (0.17 W cm^{-2} 600 s)	11 °C (in vitro)		Biocompatibility and linking availability	[56]
	GNRs@mSiO$_2$@DOX	50 × 109 nm	808 nm (3 W cm^{-2} 180 s)	6 °C (in vitro)		Chemotherapy	[57]
		68.6 × 104.6 nm	808 nm (0.5 W cm^{-2}, 60 s)	13 °C (in vivo)	29.6%	PET, PAI and chemotherapy	[58]
	GNRs@Pt	21.97 × 60.07 nm	810 nm (6 W cm^{-2} 300 s)	19.8 °C (in vivo)	94.8%	–	[59]
	GNRs@NLS	6 × 25 nm	808 nm (5.8 W cm^{-2}, 120 s)	6 °C (in vitro)		Time-dependent SERS measurement and targeted PTT	[60]
	GNRs-Cu$_7$S$_4$	20.6 × 61.4 nm	808 nm (0.9 W cm^{-2}, 254 s)	32.1 °C (aqueous solution)	62%	–	[61]
	GNRs-CuS	100.8 ± 7.5 nm	980 nm (0.9 W cm^{-2}, 300 s)	20 °C (in vivo)	61.3%	PDT, chemotherapy	[62]
	PEI-GNRs/siRNA	15 × 90 nm	808 nm (300 s)	22 °C (aqueous solution)		Gene silencing	[63]
Gold Nanospheres	NDP-MSH-PEG-HGN	43.5 nm (3–4 nm shell)	808 nm (8 W cm^{-2}, 240 s)	16.5 °C (PEG-HGN, aqueous solution)		Enhanced extravasation of agents from tumor blood vessels and dispersion into tumor	[31]
	Bumpy HGNs	46 × 56 nm	790 nm (1.0 W cm^{-2}, 300 s)	8 °C (aqueous solution)	99%	–	[32]
	Ru@GNSPs	45.0 nm	808 nm (0.8 W cm^{-2}, 300 s)	38.5 °C (aqueous solution)	33.3%	TPL imaging	[64]
Gold nanostars	GNSTs	25 nm	1064 nm (1.0 W cm^{-2}, 60 s)	5 °C (in vivo)	–		[35]
		30 nm	980 nm (0.72 W cm^{-2}, 240 s)	20 °C (in vivo)	94%	SERS, TPL, and CT	[65]
		100–150 nm	808 nm (2.0 W cm^{-2}, 100 s)	17 °C (aqueous solution)	48.4%	–	[66]
	GNSTs@Silica	100 nm (10 nm shell)	808 nm (0.5 W cm^{-2}, 600 s)	9 °C (in vivo)	–	PAI	[67]
	GSTs/ mutiwalled carbon nanotubes	60 nm (nanostars)	808 nm (1.0 W cm^{-2}, 100 s)	25 °C (aqueous solution)	–	–	[68]
Gold nanocages	GNCs	45 nm (5 nm wall)	808 nm (0.4 W cm^{-2}, 600 s)	25.8 °C (aqueous solution)	27.9%	–	[69]
	SiO$_2$/GNCs	120 ± 10 nm	808 nm (0.1238 W cm^{-2}, 600 s)	15.3 °C (aqueous solution)		SERS imaging, chemotherapy	[70]
	CoP@GNCs	100 nm	1064 nm (1.0 W cm^{-2}, 120 s)	29.1 °C (aqueous solution)	21.4%	Photoelectrochemical sensing	[71]
	Red-blood cell-coated GNCs	89.05 nm	850 nm (1.0 W cm^{-2}, 120 s)	41.5 °C (in vivo)	–	Long circulation life time	[72]
Gold nanoshells	GNSs (core Au$_2$S)	50 nm	815 nm (0.15 W, 600 s)	1.9 °C (aqueous solution)	59%	–	[73]
	GNSs	145 nm	808 nm (2.0 W cm^{-2}, 600 s)	13 °C (aqueous solution)	25%	–	[74]
	GNSs-Linear tetrapyrrole conjugates	201.9 ± 1.6 nm	800 nm (1.0 W cm^{-2}, 300 s)	25 °C (aqueous solution)	–	PDT	[46]
	Platinum(II) drug-loaded GNSs	144.3 ± 0.17 nm	808 nm (1.0 W cm^{-2}, 600 s)	18 °C (in vivo)	–	Chemotherapy	[47]
	siRNA@CPG@GNSs	30 nm	785 nm (1.2 W cm^{-2}, 300 s)	31°C (aqueous solution)	–	Immunotherapy	[75]
	Octopus-shaped gold nanoparticles	157 nm	808 nm (2.0 W cm^{-2}, 300 s)	30 °C (in vivo)	49.5%	Targeted delivery, chemotherapy	[53]
Others	Au/SiO$_2$/Au nanomatryoshkas	90 nm	810 nm (2.0 W cm^{-2}, 300 s)	33.7 °C (in vivo)	63%	–	[76]
	Gold nanoprisms	136 nm	1064 nm (5 W cm^{-2}, 600 s)	14 °C (in vitro)	–	–	[50]
	Polypyrrole-coated urchinlike gold nanoparticles	120 nm (6-nm shell)	808 nm (3 W cm^{-2}, 300 s)	23.5 °C (aqueous solution)	24%	High stability	[77]

**ADVANCED
SCIENCE NEWS**

www.advancedsciencenews.com

**ADVANCED
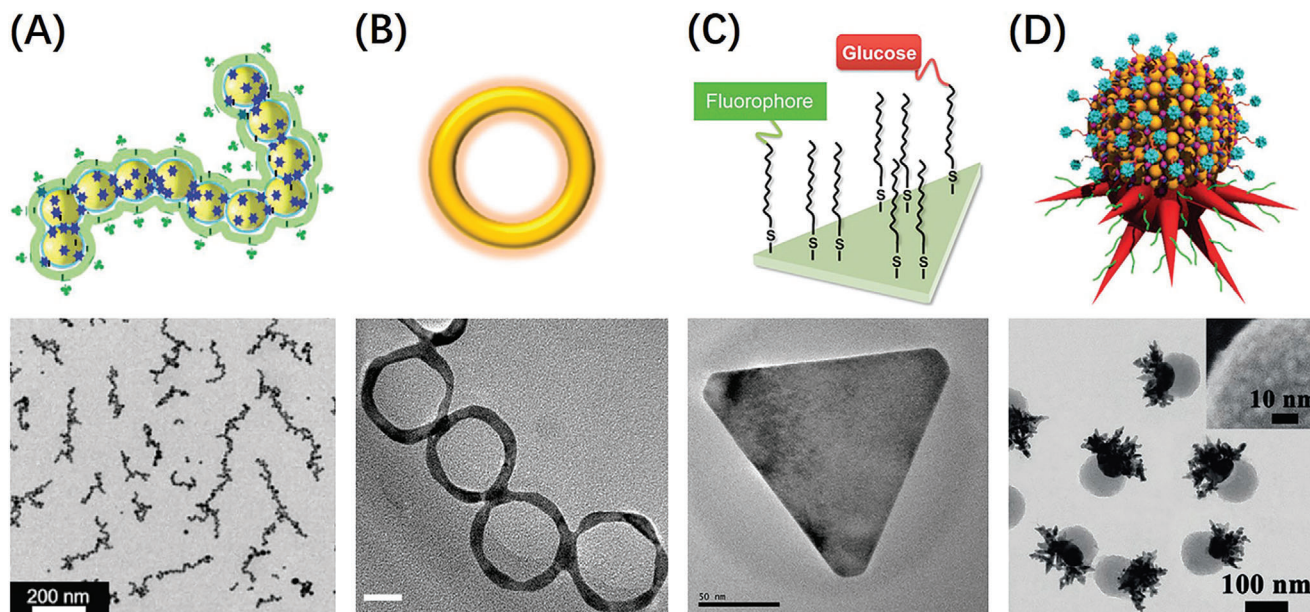HEALTHCARE
MATERIALS**

www.advhealthmat.de

Figure 5. Illustrated structures and related TEM images of recently developed gold nanomaterials used as PTT agents. A) 1D caterpillar-like gold nanoparticle assemblies with small nanogaps. B) 2D gold nanorings for enhanced cancer accumulation and PTT. C) Gold nanoprisms functionalized with glucose and 5-TAMRA cadaverine to induce cancer cell apoptosis through sharp photothermal effect. D) Octopus-type PEG-Au-PAA/mSiO₂-lactobionic acid nanoparticles for chemo-photothermal therapy. Scale bars of TEM images from left to right are 200, 20, 50, and 100 nm, respectively. (A) Reproduced with permission.[51] Copyright 2018, Wiley-VCH GmbH; (B) Reproduced with permission.[52] Copyright 2017, American Chemical Society;(C) Reproduced with permission.[50] Copyright 2015, Americna Chemical Society; (D) Repproduced with permission.[53] Copyright 2016, Wiley-VCH GmbH.

in plasmonic heating. Although gold nanomaterials have long been successfully employed for PTT, they suffered from some intrinsic drawbacks: a) relatively large size, which is inappropriate for cell intake and renal clearance,[54] b) lack of good photothermal stability upon irradiation of NIR laser,[55] and c) high cost issue.

3. Silver Nanomaterials

Renowned for their impressive antimicrobial and wound healing properties, silver nanomaterials have been extensively used as novel antimicrobial agents, detection and diagnosis platforms, tissue restoration materials as well as personal healthcare products.[78] However, only until recently silver nanomaterials have made their way to the field of PTT for cancer treatment and gained a firm foothold by virtue of low toxicity, facile preparation, metabolic nature, tunable SPR band and excellent heat conductivity superior to other metals.[79]

Generally, silver nanomaterials applied in biomedicine are spherical, with a plasmon resonance around 410 nm, which is not suitable for deep-penetrated PTT. But by developing anisotropic silver nanoparticles, the plasmon resonance can be finely tuned to NIR domain,[80] such as silver nanospheres, silver nanotriangles,[79–81] and nanocages.[82]

3.1. Silver Nanospheres

Through the reduction of hydrazine hydrate or NaBH₄, silver nitrate can well form silver nanospheres (AgNSs) with irregular

shapes and certain range of sizes around 20 nm, showing plasmonic resonance in the biologically transparent window of 650–1200 nm and light-to-heat conversion, which allows for PTT with deep tissue penetration.[83]

Two-photon absorption character of irregular AgNSs improved the efficacy of pulsed-laser-triggered PTT.[84] However, the morphology of solo AgNSs can be damaged upon femtosecond irradiation. Thus, to protect the AgNSs, organic molecules can be modified on the surface. For example, a novel flurophore-cyano-carboxylic-Ag microhybrid was developed through interfacial coordination interactions, producing a decreased fluorescence quantum yield and 13 times increase in the two-photon action cross section. Severe destruction of HeLa cells reached 82.16% after 2 min of irradiation procedure (780 nm, 2.0 W cm⁻²).[85] On the other hand, considering such mixed two-photon PTT agents may cause cytotoxicity and metabolic block, Huang et al.[86] successfully obtained an optimal silver nanohybrid (PyAnOH-Ag), featuring in combined two-photon fluorescence imaging and excellent two-photon PTT efficacy, presenting 80% photothermal cytotoxicity in vitro (HepG2 cells) and complete tumor growth inhibition in vivo. Due to SPR effect of AgNSs, the two-photon action cross section value increased from 1964 GM for PyAnOH to 4638 GM for the PyAnOH-Ag nanohybrid.

A multifunctional Mn₃[Co(CN)₆]₂@SiO₂@Ag nanocube platform was developed through coprecipitation method, combining chemo-photothermal therapy and two-photon/MRI imaging.[84] After loaded with silver, the UV–vis spectrum displayed remarkable NIR absorption and a broad peak centered at 420 nm, which attributed to the wide size distribution and diverse morphologies of AgNSs formed, as shown in **Figure 6**. The photothermal effect of AgNPs not only promote the ablation of tumor, but bring about
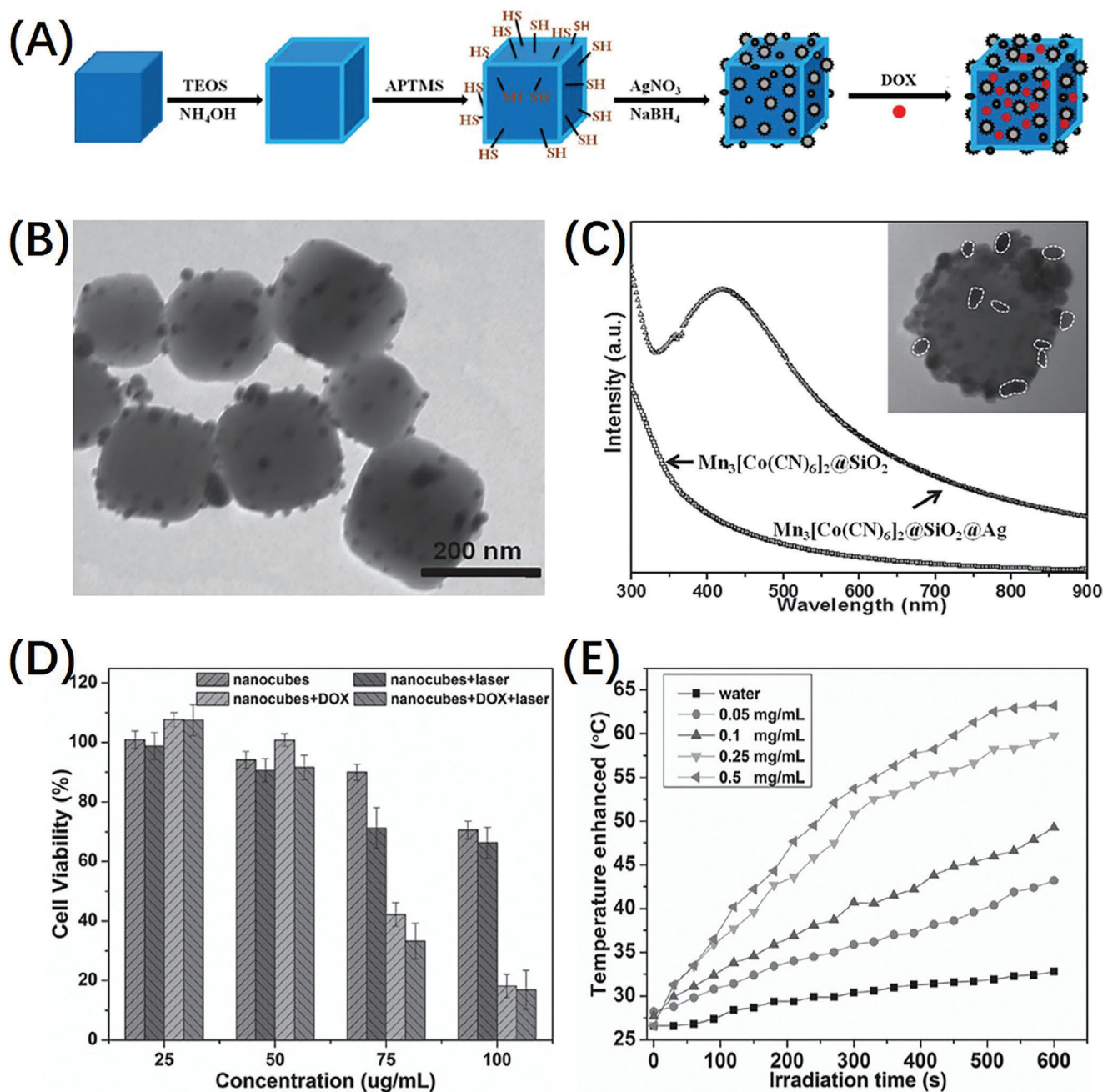
Figure 6. A) Schematic preparation process and B) SEM image of $Mn_3[Co(CN)_6]_2@SiO_2@Ag$ nanocube. C) UV–vis spectrum of $Mn_3[Co(CN)_6]_2@SiO_2$ and $Mn_3[Co(CN)_6]_2@SiO_2@Ag$. D) Cell viability test with varying concentrations of DOX-loaded nanocubes and irradiation (808 nm, 10 min, 2 W cm^{-2}). E) Temperature increase of nanocubes upon continuous irradiation (808 nm, 2 W cm^{-2}). Reproduced with permission.[84] Copyright 2015, Wiley-VCH GmbH.

DOX release for chemotherapy and enhance the TPL intensity of $Mn_3[Co(CN)_6]_2@SiO_2$ as well.

3.2. Sliver Nanotriangles

By being tailored into a triangular shape, silver nanostructures' plasmonic resonance can shift to NIR region and endow the particles with great potential as NIR-responsive photothermal agents.[79–81] Given that the corners of such silver nanotriangles (AgNTs) are highly vulnerable to oxidation, which can cause blue-shifting of the absorption and undermine photothermal effect, the coating of biopolymers, such as chitosan, are indispensable to stabilize AgNTs and additionally avoid self-aggregation as well as minimize their cytotoxicity by impeding the release of silver ions.
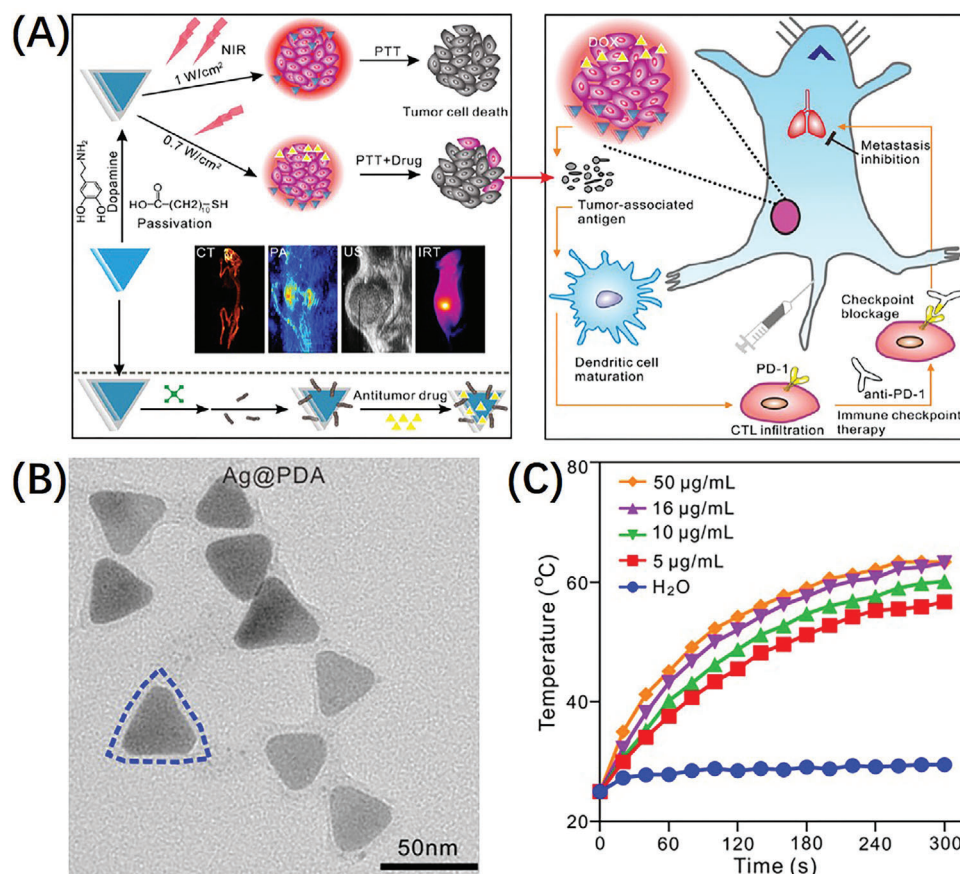
ADVANCED
SCIENCE NEWS
www.advancedsciencenews.com

ADVANCED
HEALTHCARE
MATERIALS
www.advhealthmat.de

Figure 7. A) Schematic demonstration of the preparation of the PDA-coated AgNTs nanoplatform as well as therapeutic applications. B) TEM image of PDA-coated AgNTs. C) Temperature evolution of the as-prepared PDA-coated AgNTs with different concentrations measured during laser irradiation (5 min, 808 nm, 1 W cm^{-2}). Reproduced with permission.[87] Copyright 2020, American Chemical Society.

The first employed silver nanomaterials for PTT are chitosan-coated AgNTs (Chit-AgNTs) fabricated by Boca et al. Relatively low cytotoxicity of Chit-AgNTs on healthy cells have been proved by cell viability assays combining phase contrast, fluorescence microscopy. Comparative photothermal experiments have revealed that Chit-AgNTs exhibited higher PTT efficacy at about 20 times less dose and lower laser intensities than GNRs, which could be attributed to higher cellular uptake caused by chitosan, more efficient heat conductivity for triangular-plate structure. However, the irradiation intensities applied were relatively high.[79]

Through simple self-polymerization, polydopamine (PDA) were coated on AgNTs for passivation and enhancement of biocompatibility, forming a core–shell structure which is highly potential for various strategies to achieve multifunctional PTT with other therapeutic modalities, as shown in **Figure 7**.[87] For instance, by equipping with an RGD peptide, the intelligent nanoplatform can realize antitumor drug delivery targeted at cancer cells, along with PA/IRT/CT multimodal bioimaging.

Among plasmonic materials, silver nanoparticles, were identified to have the highest activity in surface-enhanced Raman scattering (SERS), providing precise spectroscopic information regarding localization of nanoparticles.[81,88] Therefore, by labelling AgNTs with Raman reporter molecule (para-amino-thiophenol),

the photothermal cancer treatment with AgNTs is endowed with site specificity by SERS imaging and detection.[81]

3.3. Silver Nanocages

Some other distinctive types of silver nanomaterials have also come into view in recent years. Bian et al. synthesized hierarchical mineralized silver nanocages via growth process mediated by the peptide template, octreotide. Owing to the hollow nanoshell structure with ultra-strong plasmonic coupling silver nanoparticles, the silver nanocages exhibit a notably enhanced SPR and NIR absorption above 900 nm, which is ideal therapeutic window for PTT. Experiments elucidated that the PCE of silver nanocages reached 46.1% and over 82.7% tumor killing efficacy was achieved. The use of biological template rather than toxic surfactant imparted unnoticeable toxicity of the silver nanocages at the treatment dose.[82]

Silver nanomaterials with anisotropic structures exhibit strong SPR absorption in NIR region and have been used as PTT agents with good PTT efficacy. The morphologies and optical properties of silver nanomaterials need to be developed or tuned to meet the requirements of further excellent PTT efficacy and the chemical
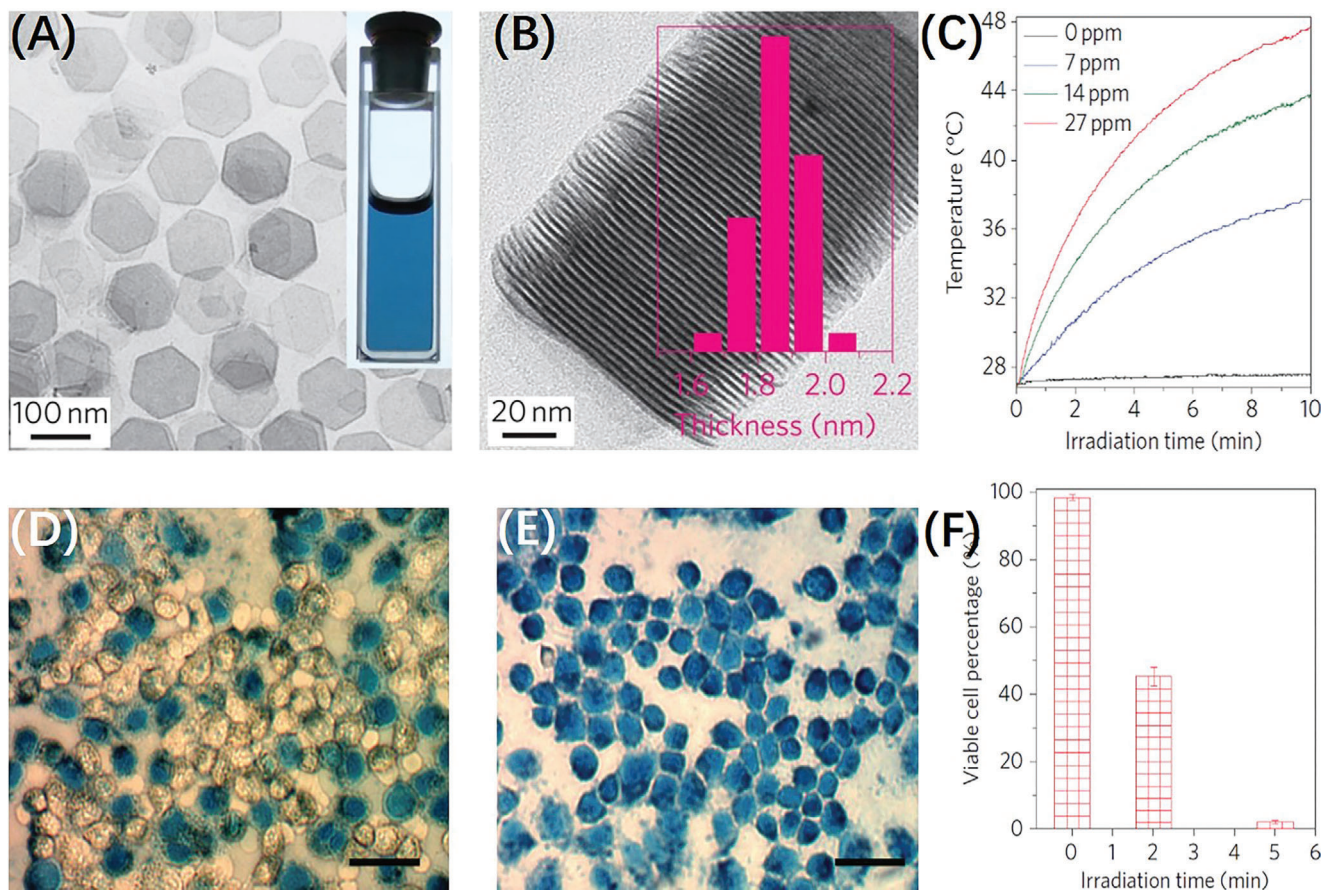
**ADVANCED
SCIENCE NEWS**

www.advancedsciencenews.com

**ADVANCED
HEALTHCARE
MATERIALS**

www.advhealthmat.de

Figure 8. Freestanding hexagonal PdNSs for PTT. A) TEM image of the PdNSs. Inset is the photo of the as-prepared PdNSs in ethanol. B) TEM image of the PdNSs situated vertical to the TEM grid. Inset is thickness distribution. C) Photothermal effect of PdNSs at different concentrations (edge length, 41 nm) upon irradiation (808 nm, 1 W cm^{-2}). D,E) Micrographs of cancer cells irradiated for 2 min (D) and 5 min (E) irradiation with scale bar = 50 μm, in which dead cells are stained with trypan blue. F) Viability of cancer cells upon laser irradiation (808 nm, 1.4 W cm^{-2}). Reproduced with permission.[90] Copyright 2011, Springer Nature.

and optical stability of silver nanomaterials is also needed to be considered.

4. Palladium Nanomaterials

In the past decade, palladium, as a low-cost noble metal, have become promising candidates for PTT agents, owing to high hyperthermia efficiency and good photothermal stability with its markedly higher bulk melting point (MP$_{Pd}$ = 1555 °C, vs MP$_{Au}$ = 1062 °C, MP$_{Ag}$ = 961 °C), thereby avoiding sharp distortion upon irradiation.[89,90]

Palladium nanosheets (PdNSs) possess high extinction coefficients in the NIR region, comparable to GNRs. Moreover, the synthetic methods of PdNSs are well-developed, green, scalable and reproducible.[91–93]

The potential of Pd nanostructures to be PTT agents was first explored by Huang et al.,[90] whose work discovered ultrathin (1.8 nm) hexagonal PdNSs, exhibiting efficient photothermal conversion with well-defined and size-dependent NIR absorption peaks. Nearly 100% death rate of cancer cells were achieved within 5 min laser irradiation at 808 nm with a power density of 1.4 W cm^{-2} as shown in **Figure 8**.

However, the 2D ultrathin feature of PdNSs hinders them from entering cells. To increase cellular internalization, Tang et al.[94] altered the sheet nature by coating PdNSs with silica, leading to thickness enhancement and facile surface functionalization. Remarkably, the uptake of PdNSs increased by 13 times at the aid of amino groups. Reversely, a nanoplatform of PdNSs-covered hollow mesoporous silica is successfully developed, also showing enhanced endocytosis by cells and NIR photothermal effect.[95]

The ultrasmall-size nature of PdNSs is beneficial to renal clearance. In the practical use of inorganic materials for PTT, optimal renal clearance is desired because it can greatly minimize the toxicity by expelling agents from human body within a proper period through renal excretion route and into urine. To achieve efficient renal clearance, the size of nanoparticles need to be below 10 nm.[96] However, few of the reported PTT nanoagents can meet the size requirement (e.g., carbon nanotubes with a length of 50–300 nm,[97] graphene with a diameter of 10–50 nm,[98] GNRs with 50 nm length,[99] GNCs with 48 nm edge length[100]), until Tang et al. successfully synthesized GSH-functionalized PdNSs with a diameter of 4.4 nm on average, well below the filtration-size threshold.[54] By comprehensive experiment

**ADVANCED
SCIENCE NEWS**

www.advancedsciencenews.com

**ADVANCED
HEALTHCARE
MATERIALS**

www.advhealthmat.de

evaluation, the ultra-small PdNSs have high PCE of 52.0% at 808 nm to ablate cancer cells, prolonged blood circulation due to surface modification with GSH, and unique renal clearance properties in vivo.

Systematic investigation into the effects of different surface ligand modification of PdNSs on the in vivo circulation biodistribution, clearance, photothermal effect and potential toxicity of PdNSs provide useful guidelines to the further exploration of Pd nanomaterials.[101] In this investigation, four biocompatible agents, namely carboxymethyl chitosan (CMC), PEG-NH$_2$, PEG-SH, and dihydrolipoic acid-zwitterion (DHLA-ZW) are explored respectively, among which PEG-SH-coated PdNSs were identified to have ultra-long in vivo circulation half-life and outstanding PTT efficacy. Certain surface ligands of PdNSs add more functionality by actively targeting at specific cell-surface receptor. PdNSs studied in a representative work[102] are functionalized with RGD peptide, which realizes targeted delivery and enhanced photothermal therapeutic effects in breast cancer cells, comparable to gold nanoparticles. The PdNSs are also modified with chitosan oligosaccharide to improve biocompatibility. What's more, the excellence of photoacoustic signals and imaging efficiency is confirmed in vitro and in vivo, thus making the PdNSs ideal nanotheranostic platforms.

There are safety concerns toward the cytotoxicity and immunogenicity of Pd species contained in Pd based PTT nanoagents, which impede further clinical application.[103–105] However, it is also stated with sufficient evidence that Pd-containing complex can achieve high biocompatibility with appropriate modification. For example, novel histidine-containing PdNSs were proved to exhibit a superior safety profile at certain concentration range, owing to the ROS scavenging properties of histidine.[93] In another case, gold nanocrystals are deposited on highly branched Pd seeds for the purpose of enhancing biocompatibility of the nanostructure, as well as boosting NIR-triggered photothermal effect.[106]

Just recently multimodal synergistic therapy is being developed for PdNSs-based PTT, and only a few reports are available. In a new paradigm of immunotherapy combined PTT, PdNSs were utilized as the vehicles of immunoadjuvant cytosine-phosphate-guanine oligodeoxynucleotides for efficient delivery as well as stimulating immune effect through photothermal performance of PdNSs with low laser power density of 0.15 W cm^{-2} at 808 nm.[107] With regard to chemo-photothermal therapy, PdNSs-crosslinked hydrogels garnered attention nowadays for it can encapsulate anticancer drug DOX, maintain high drug concentrations at the focal area with stabilized nanostructure, as mentioned in the work of Jiang et al.[108] There are also several researches focused on PdNSs-based chemo-photothermal therapy, which produced effective synergistic anticancer effect.[95,109] Interestingly, photothermally enhanced PDT is also reported. Shi et al.[110] fabricated Pd@Ag nanoparticles coated by mesoporous silica and covalently loaded with photosensitizer, Chlorin e6, showing excellent tumor suppression. Furthermore, Zhao et al. synthesized mesoporous silica nanoparticles loaded with carboxyl aluminum phthalocyanine as a photosensitizer and achieved simultaneously efficient PDT-PTT effects under 660 nm laser irradiation.[111]

More attention is devoted to PTT nanomaterials responding to NIR-II window (1000–1350 nm), under which the imaging resolution as well as light penetration depth are improved greatly.[112] To apply such advantage in PdNSs, ultra-small bimetallic Fe-Pd nanoparticles with strong NIR-II photothermal capacity and good magnetic resonance imaging were designed. By binding to macrophages, nanoparticles confine the PTT effect to intended lesion and diminish off-target toxicities greatly.[113]

Due to the good photothermal stability and optimized biomedical performances (cellular internalization, biocompatibility, renal clearance, multimodal synergistic therapy, NIR-II responsibility), palladium nanomaterials exhibited attractive prospects in PTT. Although several important aspects have been studied, the research of palladium nanomaterials as PTT agents are just at the earlier stage. The structures and optical properties of palladium nanomaterials need to be further developed or tuned to meet the requirements of clinical PTT performance.

5. Platinum Nanomaterials

Platinum has been widely used for electrocatalysis for long, and its biomedical context, especially in anticancer field, is developing rapidly as well, mostly focused on chemotherapy drugs, such as cisplatin.[114] Currently, a few researches on photothermal capability of Pt further expand its anticancer potential (**Figure 9**). The use of platinum nanoparticles (Pt NPs) in PTT possesses several outstanding advantages: 1) mild hyperthermia effect. Pt NPs generate slow and gradual temperature rise, not exceeding 46 °C upon irradiation (sufficient for triggering cell apoptosis and avoiding ablation of normal cells);[115,116] 2) resistance to photobleaching with good photostability; 3) ideal chemical and thermal stability; 4) commercial availability of high quality Pt NPs; 5) capacity to combine with chemotherapy,[117] radiotherapy,[118–120] along with photoacoustic imaging detection[119,121–123] and magnetic resonance imaging.[124,125]

Through a facile synthesis method, Pt nanoworms were prepared and exhibited both high photothermal efficiency and X-ray attenuation ability, allowing for mild PTT in the second NIR window and excellent radiotherapy as well as photoacoustic/CT imaging modalities. Pt nanoworms show uniform morphology and chemical stability in physiological. By integrating radiotherapy, effective eradication of tumor was achieved without obvious side effects, which allowed for PTT with a moderate laser intensity to avoid overheating. What's more, mild hyperthermia greatly improved the hypoxic environment of tumor, making radiotherapy favorable.[120]

To conduct repeated PTT with long agent retention time, Li et al. utilized biodegradable hydrogel formed by dendrimer-encapsulated Pt NPs crosslinked aldehyde-modified dextran via imine bond formation. The obtained Pt NPs hydrogel could remain in tumors for more than one week and will be degraded after treatment, reducing side effects caused by long-term retention. Furthermore, in vivo experiments indicated that the hydrogel degraded faster in the normal tissue. With several times of laser irradiation (808 nm, 0.54 W cm^{-2}, 5 min), tumor growth in the hydrogel group was completely inhibited, with the site temperature maintaining at ≈46°C.[126]

Zhu et al. synthesized highly compatible biopolymers, hyaluronic acid, encapsulated PtNPs, specifically bond to tumor cells overexpressing CD44 or LYVE-1, thus promoting agent internalization by cancer cells and generating effective tumor
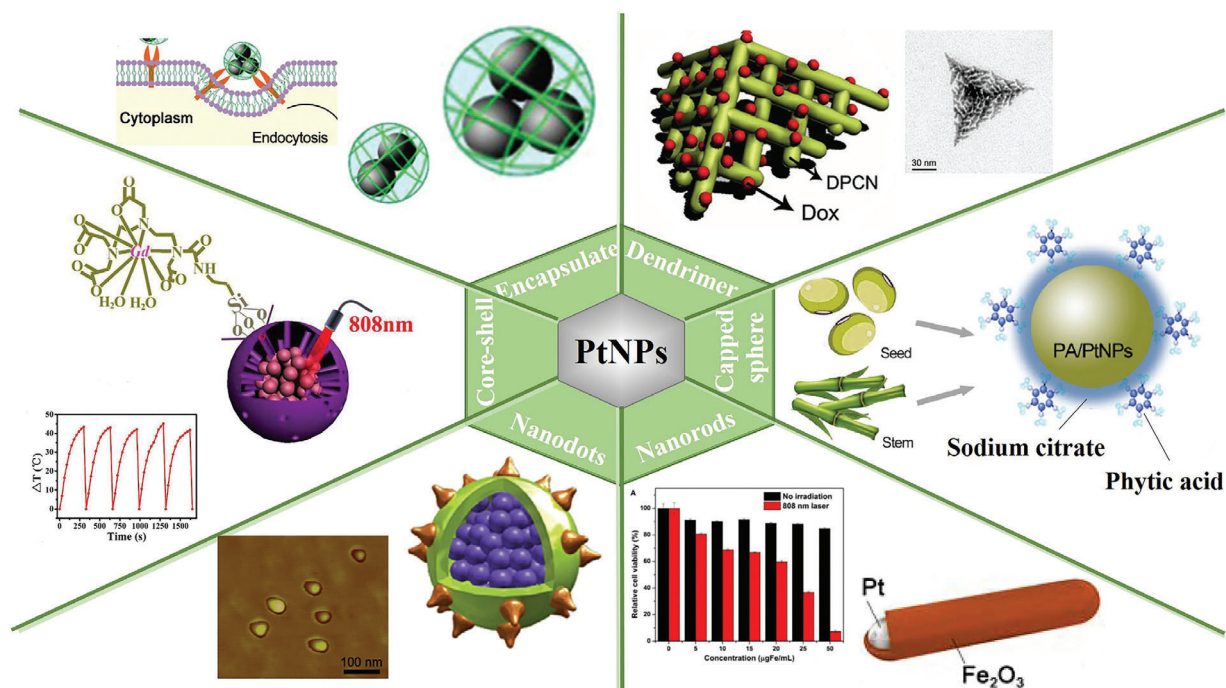
ADVANCED
SCIENCE NEWS
www.advancedsciencenews.com

ADVANCED
HEALTHCARE
MATERIALS
www.advhealthmat.de

Figure 9. Structure demonstration of recently developed platinum nanomaterials used as PTT agents. Reproduced with permission from American Scientific Publishers,[116] copyright 2017; RSC,[118] copyright 2016; Wiley-VCH,[119] copyright 2016; Elsevier,[123] copyright 2018; RSC,[124] copyright 2017; Elsevier,[127] copyright 2019.

regression.[116] Pt nanodots coordinated with albumin also possess preferable tumor accumulation. Moreover, in this study, ultrasmall size (6.7 nm) was achieved by manipulating the albumin-directed reduction and growth of tetravalent Pt ions into nanodots, thus enabling in vivo excretory capability.[123] Capped with phytic acid, Pt NPs showed high affinity to hydroxyapatite and maintained both the inherent bone-targeting ability and PTT of tumor.[127]

Novel Pt spirals, with a mono-component superstructure comprised of three levels (3D frame, 2D shell layers, and 1D nanowires), exhibit high extinction coefficients (228.7 m² mol⁻¹) and SPR wavelength extended to over 1000 nm, which lead to favorable photothermal performance in NIR-II with a high conversion efficiency up to 52.5% and deep tissue penetration. In vivo studies showed that all mice survived along with the eradication of tumor after PTT treatment, as shown in **Figure 10**.[128]

Benefiting from the strong NIR absorption and high stability, Pt NPs in several morphologies have been developed as PTT agents and exhibited good PTT efficacy. In spite of these promising studies on Pt-based PTT, there are some limitations. Present elemental Pt nanoparticles with the potential of PTT are lack of clinically approved stabilizers and shape-directing agents like dendrimers, PVP and citric.[123] On the other hand, the power intensity exerted in some Pt-based PTT studies remains relatively high, and more efficient fabrication is needed through continuous optimization.

6. Summary and Outlook

In this review, we summarized the recent development concerning the application of noble metal nanomaterials for NIR-triggered PTT. A variety of studies with good therapeutic effects against cancer from impressive photothermal efficacy of noble metal nanomaterials have been concluded. Intelligent nanoplatforms through sophisticate fabrication showing potential of multifunctional PTT, combined with chemo-therapy, immunotherapy, PDT, as well as simultaneous imaging modality were also demonstrated.

At present, the first challenge for noble metal nanomaterials in PTT is their long-term biological behavior. Despite their excellent photothermal efficacy, they are still suffering from tough biodegradation and potential toxicity, which can cause severe side effects, such as long-term accumulation in organs. Moreover, some clinically unacceptable ingredient, such as harsh surfactants like CTAB, are used in synthesis and post-modifications, if not removed completely, could be deleterious to human body as well.[129] Thus, further investigation concerning pharmacokinetics, biodistribution and toxicity of noble metal PTT agents are highly demanded.

Another challenge is to overcome the physical limitation of light penetration depth, which is usually less than 1 cm under the skin, leaving the deep-situated tumors beyond effective PTT treatment. To overcome the hurdle, possible solutions are as follows: 1) Develop NIR-II-responsive PTT.[130] Considering the longer-length light in the NIR II window (1000–1350 nm) has a less tissue absorption, thus deeper tissue penetration, it is reasonable to fabricate PTT nanomaterials that can be triggered by NIR-II laser. Plus, compared to the traditional NIR-I PTT, NIR-II responsive PTT has a higher MPE (maximum permissible exposure) (1.0 W cm⁻²), which makes more materials available for safe application.[131] 2) Employ two and more photon laser source. Studies proved that pulsed femtosecond laser in PTT was more
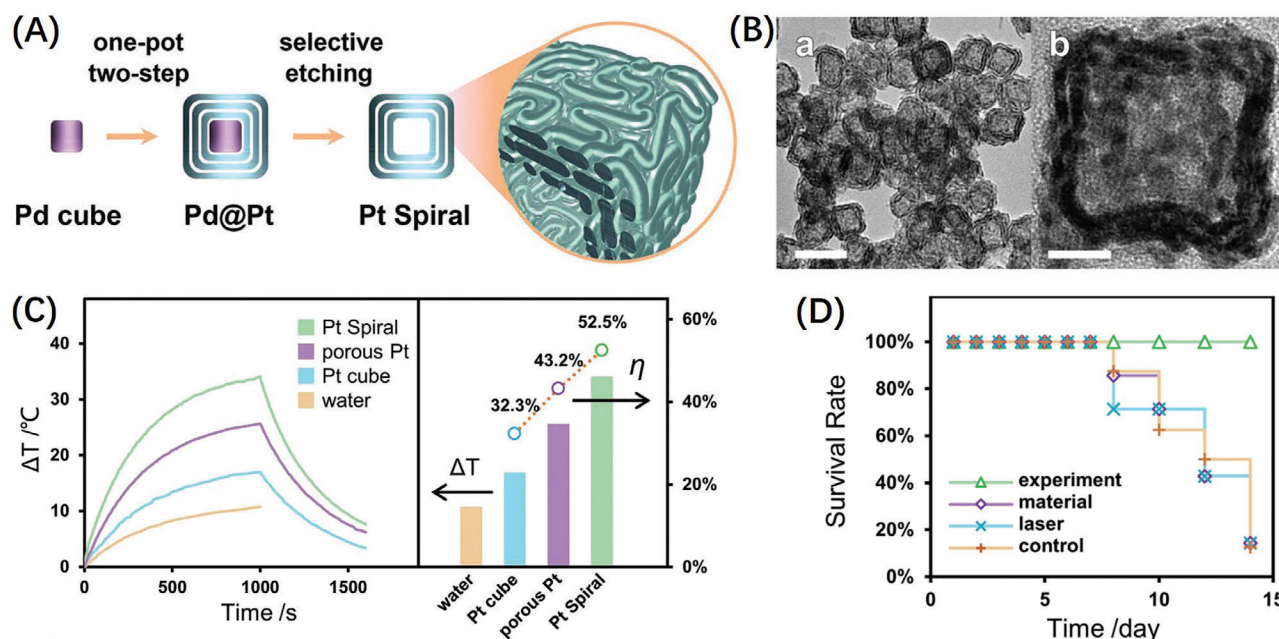
Figure 10. A) Schematic demonstration of the synthesis and multilevel structure of Pt spirals. B) TEM images of Pt spirals. Scale bars = 50 nm (a), 10 nm (b). C) Temperature evolution curves, temperature difference (ΔT), PCE (η) of Pt spiral, porous Pt, Pt cube, and water. D) Survival rate of mice bearing tumor after varying treatments. Reproduced with permission.[128] Copyright 2019, American Chemical Society.

effective than continuous wave laser, because of deeper tissue penetration derived from low Rayleigh scattering and minimized tissue absorption of NIR light, as well as low background signal, reduced photobleaching, and photo toxicity.[132,133] 3) Using other external fields to stimulate the PTT process. Just like radiodynamic therapy (RDT)[134] or sonodynamic therapy (SDT)[135,136] using X-ray or ultrasound with deep penetration to trigger the generation of ROS, the PTT can also be triggered by other external fields through exquisite design. 4) Get rid of external fields. By drawing a reference from dark-photodynamic therapy (dPDT)[137] or chemodynamic therapy (CDT),[138] which uses chemical reaction to excite photosensitizers or generate ROS, the irradiation of laser that provides energy to stimulate PTT agents can be replaced by chemical reactions in which the released energy can be converted by PTT agents to heat as well.

The transition from bench to clinic of noble metal nanomaterials deserves further detailed and rounded investigation. Among them, the earliest gold nanomaterials are gradually extending from in vivo/in vitro studies to clinical trials as PTT agents, while silver, palladium and platinum nanomaterials are still at their infancy stage, with more structural and functional possibility to be explored.

Acknowledgements

Conflict of Interest

The authors declare no conflict of interest.

Keywords

[1] Z. Li, S. Tan, S. Li, Q. Shen, K. Wang, *Oncol. Rep.* **2017**, *38*, 611.
[2] F. Bray, J. Ferlay, I. Soerjomataram, R. L. Siegel, A. Torre, A. Jemal, *Ca-Cancer J. Clin.* **2018**, *68*, 394.
[3] E. Pérez-Herrero, A. Fernández-Medarde, *Eur. J. Pharm. Biopharm.* **2015**, *93*, 52.
[4] N. J. Curtin, *Nat. Rev. Cancer* **2012**, *12*, 801.
[5] M. Baumann, M. Krause, R. Hill, *Nat. Rev. Cancer* **2008**, *8*, 545.
[6] A. Kalbasi, C. Komar, G. M. Tooker, M. Liu, J. W. Lee, W. L. Gladney, E. Ben-Josef, G. L. Beatty, *Clin. Cancer Res.* **2017**, *23*, 137.
[7] Q. Ban, T. Bai, X. Duan, J. Kong, *Biomater. Sci.* **2017**, *5*, 190.
[8] L. Zou, H. Wang, B. He, L. Zeng, T. Tan, H. Cao, X. He, Z. Zhang, S. Guo, Y. Li, *Theranostics* **2016**, *6*, 762.
[9] Y. Liu, P. Bhattarai, Z. Dai, X. Chen, *Chem. Soc. Rev.* **2019**, *48*, 2053.
[10] G. Kong, R. D. Braun, M. W. Dewhirst, *Cancer Res.* **2001**, *61*, 3027.
[11] Y. W. Chen, Y. L. Su, S. H. Hu, S. Y. Chen, *Adv. Drug Delivery Rev.* **2016**, *105*, 190.
[12] Z. Tang, H. Zhang, Y. Liu, D. Ni, H. Zhang, J. Zhang, Z. Yao, M. He, J. Shi, W. Bu, *Adv. Mater.* **2017**, *29*, 1701683.
[13] L. Sun, Z. Li, R. Su, Y. Wang, Z. Li, B. Du, Y. Sun, P. Guan, F. Besenbacher, M. Yu, *Angew. Chem., Int. Ed.* **2018**, *57*, 10666.

**ADVANCED
SCIENCE NEWS**

www.advancedsciencenews.com

**ADVANCED
HEALTHCARE
MATERIALS**

www.advhealthmat.de

[14] Q. Xiao, X. Zheng, W. Bu, W. Ge, S. Zhang, F. Chen, H. Xing, Q. Ren, W. Fan, K. Zhao, *J. Am. Chem. Soc.* **2013**, *135*, 13041.

[15] C. Xie, W. Zhou, Z. Zeng, Q. Fan, K. Pu, *Chem. Sci.* **2020**, *11*, 10553.

[16] W. Zhang, W. Deng, H. Zhang, X. Sun, T. Huang, W. Wang, P. Sun, Q. Fan, W. Huang, *Biomaterials* **2020**, *243*, 119934.

[17] X. Huang, P. K. Jain, I. H. El-Sayed, M. A. El-Sayed, *Lasers Med. Sci.* **2008**, *23*, 217.

[18] M. Kim, J.-H. Lee, J.-M. Nam, *Adv. Sci.* **2019**, *6*, 1900471.

[19] J. Conde, G. Doria, P. Baptista, *J. Drug Delivery* **2012**, *2012*, 1.

[20] F. Jabeen, M. Najam-ul-Haq, R. Javeed, C. W. Huck, G. K. Bonn, *Molecules* **2014**, *19*, 20580.

[21] L. Pan, J. Liu, J. Shi, *ACS Appl. Mater. Interfaces* **2017**, *9*, 15952.

[22] C. Sönnichsen, T. Franzl, T. Wilk, G. von Plessen, J. Feldmann, O. Wilson, P. Mulvaney, *Phys. Rev. Lett.* **2002**, *88*, 077402.

[23] B. Jang, J.-Y. Park, C.-H. Tung, I.-H. Kim, Y. Choi, *ACS Nano* **2011**, *5*, 1086.

[24] V. P. Chauhan, Z. Popović, O. Chen, J. Cui, D. Fukumura, M. G. Bawendi, R. K. Jain, *Angew. Chem., Int. Ed.* **2011**, *50*, 11417.

[25] S. Kessentini, D. Barchiesi, *Biomed. Opt. Express* **2012**, *3*, 590.

[26] L. Vigderman, B. P. Khanal, E. R. Zubarev, *Adv. Mater.* **2012**, *24*, 4811.

[27] X. Huang, I. H. El-Sayed, W. Qian, M. A. El-Sayed, *J. Am. Chem. Soc.* **2006**, *128*, 2115.

[28] Z. Li, H. Huang, S. Tang, Y. Li, X.-F. Yu, H. Wang, P. Li, Z. Sun, H. Zhang, C. Liu, *Biomaterials* **2016**, *74*, 144.

[29] X. Huang, W. Qian, I. H. El-Sayed, M. A. El-Sayed, *Lasers Surg. Med.* **2007**, *39*, 747.

[30] J. Z. Zhang, *J. Phys. Chem. Lett.* **2010**, *1*, 686.

[31] W. Lu, C. Xiong, G. Zhang, Q. Huang, R. Zhang, J. Z. Zhang, C. Li, *Clin. Cancer Res.* **2009**, *15*, 876.

[32] S. A. Lindley, J. Z. Zhang, *ACS Appl. Nano Mater.* **2019**, *2*, 1072.

[33] E. T. Vickers, M. Garai, S. Bonabi Naghadeh, S. Lindley, J. Hibbs, Q.-H. Xu, J. Z. Zhang, *J. Phys. Chem. C* **2018**, *122*, 13304.

[34] W. Zhao, J. M. Karp, *Nat. Mater.* **2009**, *8*, 453.

[35] A. Espinosa, A. K. Silva, A. Sánchez-Iglesias, M. Grzelczak, C. Péchoux, K. Desboeufs, L. M. Liz-Marzán, C. Wilhelm, *Adv. Healthcare Mater.* **2016**, *5*, 1040.

[36] H. Yuan, A. M. Fales, T. Vo-Dinh, *J. Am. Chem. Soc.* **2012**, *134*, 11358.

[37] J. Chen, C. Glaus, R. Laforest, Q. Zhang, M. Yang, M. Gidding, M. J. Welch, Y. Xia, *Small* **2010**, *6*, 811.

[38] M. S. Yavuz, Y. Cheng, J. Chen, C. M. Cobley, Q. Zhang, M. Rycenga, J. Xie, C. Kim, K. H. Song, A. G. Schwartz, *Nat. Mater.* **2009**, *8*, 935.

[39] J.-G. Piao, F. Gao, Y. Li, L. Yu, D. Liu, Z.-B. Tan, Y. Xiong, L. Yang, Y.-Z. You, *Nano Res.* **2018**, *11*, 3193.

[40] Z. Wang, Z. Chen, Z. Liu, P. Shi, K. Dong, E. Ju, J. Ren, X. Qu, *Biomaterials* **2014**, *35*, 9678.

[41] T. S. Hauck, W. C. Chan, *Nanomedicine* **2007**, *2*, 735.

[42] N. K. Grady, N. J. Halas, P. Nordlander, *Chem. Phys. Lett.* **2004**, *399*, 167.

[43] A. R. Lowery, A. M. Gobin, E. S. Day, N. J. Halas, J. L. West, *Int. J. Nanomed.* **2006**, *1*, 149.

[44] H. Ghaznavi, S. Hosseini-Nami, S. K. Kamrava, R. Irajirad, S. Maleki, A. Shakeri-Zadeh, A. Montazerabadi, *Artif. Cells, Nanomed., Biotechnol.* **2018**, *46*, 1594.

[45] A. M. Schwartzberg, J. Z. Zhang, *J. Phys. Chem. C* **2008**, *112*, 10323.

[46] J. Wang, A. M. Potocny, J. Rosenthal, E. S. Day, *ACS Omega* **2020**, *5*, 926.

[47] S.-Y. Lee, M.-J. Shieh, *ACS Appl. Mater. Interfaces* **2020**, *12*, 4254.

[48] F. Chen, W. Cai, *Nanomedicine* **2015**, *10*, 1.

[49] A. R. Rastinehad, H. Anastos, E. Wajswol, J. S. Winoker, J. P. Sfakianos, S. K. Doppalapudi, M. R. Carrick, C. J. Knauer, B. Taouli, S. C. Lewis, A. K. Tewari, J. A. Schwartz, S. E. Canfield, A. K. George, J. L. West, N. J. Halas, *Proc. Natl. Acad. Sci. USA* **2019**, *116*, 18590.

[50] M. Pérez-Hernández, P. del Pino, S. G. Mitchell, M. Moros, G. Stepien, B. Pelaz, W. J. Parak, E. M. Gálvez, J. Pardo, J. M. de la Fuente, *ACS Nano* **2015**, *9*, 52.

[51] Y. Xia, X. Ma, J. Gao, G. Chen, Z. Li, X. Wu, Z. Yu, J. Xing, L. Sun, H. Ruan, L. Luo, L. Xiang, C. Dong, W. Ren, Z. Shen, A. Wu, *Small* **2018**, *14*, 1800094.

[52] Y. Liu, Z. Wang, Y. Liu, G. Zhu, O. Jacobson, X. Fu, R. Bai, X. Lin, N. Lu, X. Yang, W. Fan, J. Song, Z. Wang, G. Yu, F. Zhang, H. Kalish, G. Niu, Z. Nie, X. Chen, *ACS Nano* **2017**, *11*, 10539.

[53] L. Zhang, Y. Chen, Z. Li, L. Li, P. Saint-Cricq, C. Li, J. Lin, C. Wang, Z. Su, J. I. Zink, *Angew. Chem., Int. Ed.* **2016**, *55*, 2118.

[54] S. Tang, M. Chen, N. Zheng, *Small* **2014**, *10*, 3139.

[55] C. B. S. Link, M. B. Mohamed, B. Nikoobakht, M. A. El-Sayed, *J. Phys. Chem. A* **1999**, *103*, 1165.

[56] Y. V. Kaneti, C. Chen, M. Liu, X. Wang, J. L. Yang, R. A. Taylor, X. Jiang, A. Yu, *ACS Appl. Mater. Interfaces* **2015**, *7*, 25658.

[57] H. Tang, S. Shen, J. Guo, B. Chang, X. Jiang, W. Yang, *J. Mater. Chem.* **2012**, *22*, 16095.

[58] C. Xu, F. Chen, H. F. Valdovinos, D. Jiang, S. Goel, B. Yu, H. Sun, T. E. Barnhart, J. J. Moon, W. Cai, *Biomaterials* **2018**, *165*, 56.

[59] J. Tang, X. Jiang, L. Wang, H. Zhang, Z. Hu, Y. Liu, X. Wu, C. Chen, *Nanoscale* **2014**, *6*, 3670.

[60] M. R. Ali, Y. Wu, T. Han, X. Zang, H. Xiao, Y. Tang, R. Wu, F. M. Fernández, M. A. El-Sayed, *J. Am. Chem. Soc.* **2016**, *138*, 15434.

[61] C. Leng, X. Zhang, F. Xu, Y. Yuan, H. Pei, Z. Sun, L. Li, Z. Bao, *Small* **2018**, *14*, 1703077.

[62] Y. Chang, Y. Cheng, Y. Feng, H. Jian, L. Wang, X. Ma, X. Li, H. Zhang, *Nano Lett.* **2018**, *18*, 886.

[63] J. Shen, H. C. Kim, C. Mu, E. Gentile, J. Mai, J. Wolfram, L. n. Ji, M. Ferrari, Z. w. Mao, H. Shen, *Adv. Healthcare Mater.* **2014**, *3*, 1629.

[64] P. Zhang, J. Wang, H. Huang, B. Yu, K. Qiu, J. Huang, S. Wang, L. Jiang, G. Gasser, L. Ji, *Biomaterials* **2015**, *63*, 102.

[65] Y. Liu, J. R. Ashton, E. J. Moding, H. Yuan, J. K. Register, A. M. Fales, J. Choi, M. J. Whitley, X. Zhao, Y. Qi, *Theranostics* **2015**, *5*, 946.

[66] D. Wu, M. Fan, L. Y. Zhang, J. J. Xing, S. F. Lyu, L. Y. Zeng, *Faguang Xuebao* **2018**, *39*, 280.

[67] V. Raghavan, C. O'Flatharta, R. Dwyer, A. Breathnach, H. Zafar, P. Dockery, A. Wheatley, I. Keogh, M. Leahy, M. Olivo, *Nanomedicine* **2017**, *12*, 457.

[68] Y. Zhu, Q. Sun, Y. Liu, T. Ma, L. Su, S. Liu, X. Shi, D. Han, F. Liang, *R. Soc. Open Sci.* **2018**, *5*, 180159.

[69] J. Zeng, D. Goldfeld, Y. Xia, *Angew. Chem., Int. Ed.* **2013**, *52*, 4169.

[70] F. Hu, Y. Zhang, G. Chen, C. Li, Q. Wang, *Small* **2015**, *11*, 985.

[71] J. Tian, H. Zhu, J. Chen, X. Zheng, H. Duan, K. Pu, P. Chen, *Small* **2017**, *13*, 1700798.

[72] J.-G. Piao, L. Wang, F. Gao, Y.-Z. You, Y. Xiong, L. Yang, *ACS Nano* **2014**, *8*, 10414.

[73] J. R. Cole, N. A. Mirin, M. W. Knight, G. P. Goodrich, N. J. Halas, *J. Phys. Chem. C* **2009**, *113*, 12090.

[74] V. P. Pattani, J. W. Tunnell, *Lasers Surg. Med.* **2012**, *44*, 675.

[75] J. Zhang, T. Zhao, F. Han, Y. Hu, Y. Li, *J. Nanobiotechnol.* **2019**, *17*, 80.

[76] C. Ayala-Orozco, C. Urban, M. W. Knight, A. S. Urban, O. Neumann, S. W. Bishnoi, S. Mukherjee, A. M. Goodman, H. Charron, T. Mitchell, M. Shea, R. Roy, S. Nanda, R. Schiff, N. J. Halas, A. Joshi, *ACS Nano* **2014**, *8*, 6372.

[77] J. Li, J. Han, T. Xu, C. Guo, X. Bu, H. Zhang, L. Wang, H. Sun, B. Yang, *Langmuir* **2013**, *29*, 7102.

[78] A.-C. Burdusel, O. Gherasim, A. M. Grumezescu, L. Mogoantă, A. Ficai, E. Andronescu, *Nanomaterials* **2018**, *8*, 681.

[79] S. C. Boca, M. Potara, A. M. Gabudean, A. Juhem, P. L. Baldeck, S. Astilean, *Cancer Lett.* **2011**, *311*, 131.

[80] E. A. Thompson, E. Graham, C. M. MacNeill, M. Young, G. Donati, E. M. Wailes, B. T. Jones, N. H. Levi-Polyachenko, *Int. J. Hyperthermia* **2014**, *30*, 312.

[81] S. Boca-Farcau, M. Potara, T. Simon, A. Juhem, P. Baldeck, S. Astilean, *Mol. Pharmaceutics* **2014**, *11*, 391.

[82] K. Bian, X. Zhang, K. Liu, T. Yin, H. Liu, K. Niu, W. Cao, D. Gao, *ACS Sustainable Chem. Eng.* **2018**, *6*, 7574.

[83] P. Bose, A. Priyam, R. Kar, S. P. Pattanayak, *RSC Adv.* **2020**, *10*, 31961.

[84] D. Wang, Z. Guo, J. Zhou, J. Chen, G. Zhao, R. Chen, M. He, Z. Liu, H. Wang, Q. Chen, *Small* **2015**, *11*, 5956.

[85] L. Kong, L. Yang, C. Q. Xin, S. J. Zhu, H. H. Zhang, M. Z. Zhang, J. X. Yang, L. Li, H. P. Zhou, Y. P. Tian, *Biosens. Bioelectron.* **2018**, *108*, 14.

[86] Z. Huang, L. Gao, L. Kong, H. H. Zhang, J. X. Yang, L. Li, *J. Mater. Chem. B* **2019**, *7*, 7377.

[87] X. Zeng, S. Yan, C. Di, M. Lei, P. Chen, W. Du, Y. Jin, B.-F. Liu, *ACS Appl. Mater. Interfaces* **2020**, *12*, 11329.

[88] L. A. Austin, M. A. Mackey, E. C. Dreaden, M. A. El-Sayed, *Arch. Toxicol.* **2014**, *88*, 1391.

[89] A. Dumas, P. Couvreur, *Chem. Sci.* **2015**, *6*, 2153.

[90] X. Huang, S. Tang, X. Mu, Y. Dai, G. Chen, Z. Zhou, F. Ruan, Z. Yang, N. Zheng, *Nat. Nanotechnol.* **2011**, *6*, 28.

[91] K. Anand, C. Tiloke, A. Phulukdaree, B. Ranjan, A. Chuturgoon, S. Singh, R. M. Gengan, *J. Photochem. Photobiol., B* **2016**, *165*, 87.

[92] S. Gurunathan, E. Kim, J. W. Han, J. H. Park, J. H. Kim, *Molecules* **2015**, *20*, 22476.

[93] B. Rubio-Ruiz, A. M. Perez-Lopez, T. L. Bray, M. Lee, A. Serrels, M. Prieto, M. Arruebo, N. O. Carragher, V. Sebastian, A. Unciti-Broceta, *ACS Appl. Mater. Interfaces* **2018**, *10*, 3341.

[94] S. Tang, X. Huang, N. Zheng, *Chem. Commun.* **2011**, *47*, 3948.

[95] W. Fang, S. Tang, P. Liu, X. Fang, J. Gong, N. Zheng, *Small* **2012**, *8*, 3816.

[96] P. L. C. M. Longmire, H. Kobayashi, *Nanomedicine* **2008**, *3*, 703.

[97] J. T. Robinson, K. Welsher, S. M. Tabakman, S. P. Sherlock, H. Wang, R. Luong, H. Dai, *Nano Res.* **2010**, *3*, 779.

[98] A. M. Gobin, M. H. Lee, N. J. Halas, W. D. James, R. A. Drezek, J. L. West, *Nano Lett.* **2007**, *7*, 1929.

[99] M. A. E.-S. B. Nikoobakht, *Chem. Mater.* **2003**, *15*, 1957.

[100] J. W. Xiao, S. X. Fan, F. Wang, L. D. Sun, X. Y. Zheng, C. H. Yan, *Nanoscale* **2014**, *6*, 4345.

[101] S. Shi, Y. Huang, X. Chen, J. Weng, N. Zheng, *ACS Appl. Mater. Interfaces* **2015**, *7*, 14369.

[102] S. Bharathiraja, N. Q. Bui, P. Manivasagan, M. S. Moorthy, S. Mondal, H. Seo, N. T. Phuoc, T. T. Vy Phan, H. Kim, K. D. Lee, J. Oh, *Sci. Rep.* **2018**, *8*, 500.

[103] A. Nel, T. Xia, L. Madler, N. Li, *Science* **2006**, *311*, 622.

[104] L. Fontana, V. Leso, A. Marinaccio, G. Cenacchi, V. Papa, K. Leopold, R. Schindl, B. Bocca, A. Alimonti, I. Iavicoli, *Nanotoxicology* **2015**, *9*, 843.

[105] I. Iavicoli, L. Fontana, M. Corbi, V. Leso, A. Marinaccio, K. Leopold, R. Schindl, A. Sgambato, *PLoS One* **2015**, *10*, 0143801.

[106] A. J. McGrath, Y. H. Chien, S. Cheong, D. A. Herman, J. Watt, A. M. Henning, L. Gloag, C. S. Yeh, R. D. Tilley, *ACS Nano* **2015**, *9*, 12283.

[107] J. Ming, J. Zhang, Y. Shi, W. Yang, J. Li, D. Sun, S. Xiang, X. Chen, L. Chen, N. Zheng, *Nanoscale* **2020**, *12*, 3916.

[108] Y. W. Jiang, G. Gao, P. Hu, J. B. Liu, Y. Guo, X. Zhang, X. W. Yu, F. G. Wu, X. Lu, *Nanoscale* **2020**, *12*, 210.

[109] S. Tang, M. Chen, N. Zheng, *Nano Res.* **2015**, *8*, 165.

[110] S. Shi, X. Zhu, Z. Zhao, W. Fang, M. Chen, Y. Huang, X. Chen, *J. Mater. Chem. B* **2013**, *1*, 1133.

[111] Z. Zhao, S. Shi, Y. Huang, S. Tang, X. Chen, *ACS Appl. Mater. Interfaces* **2014**, *6*, 8878.

[112] X. Yu, A. Li, C. Zhao, K. Yang, X. Chen, W. Li, *ACS Nano* **2017**, *11*, 3990.

[113] Y. Yang, M. Lyu, J.-H. Li, D.-M. Zhu, Y.-F. Yuan, W. Liu, *RSC Adv.* **2019**, *9*, 33378.

[114] T. C. Johnstone, K. Suntharalingam, S. J. Lippard, *Chem. Rev.* **2016**, *116*, 3436.

[115] D. Chen, S. Gao, W. Ge, Q. Li, H. Jiang, X. Wang, *RSC Adv.* **2014**, *4*, 40141.

[116] Y. Zhu, W. Li, X. Zhao, Z. Zhou, Y. Wang, Y. Cheng, Q. Huang, Q. Zhang, *J. Biomed. Nanotechnol.* **2017**, *13*, 1457

[117] H. Zhao, J. Xu, W. Huang, G. Zhan, Y. Zhao, H. Chen, X. Yang, *ACS Nano* **2019**, *13*, 6647.

[118] Y. Deng, E. Li, X. Cheng, J. Zhu, S. Lu, C. Ge, H. Gu, Y. Pan, *Nanoscale* **2016**, *8*, 3895.

[119] Z. Zhou, K. Hu, R. Ma, Y. Yan, B. Ni, Y. Zhang, L. Wen, Q. Zhang, Y. Cheng, *Adv. Funct. Mater.* **2016**, *26*, 5971.

[120] Q. Ma, L. Cheng, F. Gong, Z. Dong, C. Liang, M. Wang, L. Feng, Y. Li, Z. Liu, C. Li, L. He, *J. Mater. Chem. B* **2018**, *6*, 5069.

[121] D. Y. Lee, J. Y. Kim, Y. Lee, S. Lee, W. Miao, H. S. Kim, J. J. Min, S. Jon, *Angew. Chem., Int. Ed.* **2017**, *56*, 13684.

[122] T. T. V. Phan, N. Q. Bui, M. S. Moorthy, K. D. Lee, J. Oh, *Nanoscale Res. Lett.* **2017**, *12*, 570.

[123] Y. Tang, T. Yang, Q. Wang, X. Lv, X. Song, H. Ke, Z. Guo, X. Huang, J. Hu, Z. Li, P. Yang, X. Yang, H. Chen, *Biomaterials* **2018**, *154*, 248.

[124] L. Zhao, X. Ge, G. Yan, X. Wang, P. Hu, L. Shi, O. S. Wolfbeis, H. Zhang, L. Sun, *Nanoscale* **2017**, *9*, 16012.

[125] C. L. Chen, L. R. Kuo, S. Y. Lee, Y. K. Hwu, S. W. Chou, C. C. Chen, F. H. Chang, K. H. Lin, D. H. Tsai, Y. Y. Chen, *Biomaterials* **2013**, *34*, 1128.

[126] L. Li, C. Wang, Q. Huang, J. Xiao, Q. Zhang, Y. Cheng, *J. Mater. Chem. B* **2018**, *6*, 2474.

[127] Z. Zhou, T. Fan, Y. Yan, S. Zhang, Y. Zhou, H. Deng, X. Cai, J. Xiao, D. Song, Q. Zhang, Y. Cheng, *Biomaterials* **2019**, *194*, 130.

[128] Q. Wang, H. Wang, Y. Yang, L. Jin, Y. Liu, Y. Wang, X. Yan, J. Xu, R. Gao, P. Lei, J. Zhu, Y. Wang, S. Song, H. Zhang, *Adv. Mater.* **2019**, *31*, 1904836.

[129] M. R. K. Ali, Y. Wu, M. A. El-Sayed, *J. Phys. Chem. C* **2019**, *123*, 15375.

[130] E. D. Onal, K. Guven, *J. Phys. Chem. C* **2017**, *121*, 684.

[131] Y. Liu, W. Zhen, Y. Wang, J. Liu, L. Jin, T. Zhang, S. Zhang, Y. Zhao, S. Song, C. Li, J. Zhu, Y. Yang, H. Zhang, *Angew. Chem., Int. Ed.* **2019**, *58*, 2407.

[132] J. L. Li, H. C. Bao, X. L. Hou, L. Sun, X. G. Wang, M. Gu, *Angew. Chem., Int. Ed.* **2012**, *51*, 1830.

[133] J. L. Li, D. Day, M. Gu, *Adv. Mater.* **2008**, *20*, 3866.

[134] K. Lu, C. He, N. Guo, C. Chan, K. Ni, G. Lan, H. Tang, C. Pelizzari, Y.-X. Fu, M. T. Spiotto, R. R. Weichselbaum, W. Lin, *Nat. Biomed. Eng.* **2018**, *2*, 600.

[135] J. Ouyang, Z. Tang, N. Farokhzad, N. Kong, N. Y. Kim, C. Feng, S. Blake, Y. Xiao, C. Liu, T. Xie, W. Tao, *Nano Today* **2020**, *35*, 100949.

[136] X. Pan, H. Wang, S. Wang, X. Sun, L. Wang, W. Wang, H. Shen, H. Liu, *Sci. China: Life Sci.* **2018**, *61*, 415.

[137] D. Mao, W. Wu, S. Ji, C. Chen, F. Hu, D. Kong, D. Ding, B. Liu, *Chem* **2017**, *3*, 991.

[138] Z. Tang, Y. Liu, M. He, W. Bu, *Angew. Chem., Int. Ed.* **2019**, *58*, 946.

ADVANCED
SCIENCE NEWS

www.advancedsciencenews.com

ADVANCED
HEALTHCARE
MATERIALS

www.advhealthmat.de
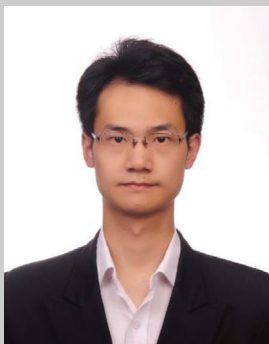
Youfu Wang received his B.Sc. and Ph.D. degrees from East China University of Science and Technology in China. Then, he did his postdoctoral research in Shanghai Jiao Tong University (SJTU). Now, he is a research associate in School of Chemistry and Chemical Engineering at SJTU. His research interests focus on polymer directed nanofabrication, ordered nanomaterials in low dimensions, and novel strategies for cancer therapy.

Xinyuan Zhu completed his B.Sc. and M.Sc. degrees at Donghua University, and obtained his Ph.D. degree from Shanghai Jiao Tong University in China. Then, he did his postdoctoral research in the BASF laboratory of ISIS at Strasbourg. He was promoted to a full professor for chemistry at Shanghai Jiao Tong University in 2005. His research interests focus on the controlled preparation of functional polymers and their biomedical applications.